Presented at
STRUCTURES DESIGN CONFERENCE '97
Florida Department of Transportation, Florida, USA
July21st -23rd, 1997

DESIGN FUNDAMENTALS OF SEGMENTALLY CONSTRUCTED BRIDGES

with Particular Reference to AASHTO LRFD Method

Bijan O Aalami[1], PhD SE

June 10, 1997

ABSTRACT:

New technology in construction, coupled with increased application of high performance concrete, has opened new opportunities for segmentally constructed bridges, in particular prestressed precast girders spliced for continuity and topped with a concrete slab. High strength concrete, early age loading, segmental construction, composite action, and the combination of pre-and post-tensioning, pose a challenge to the structural engineer in computation of alignment during the construction phase, camber and final deformation of the structure and determination of actions for serviceability and strength checks. This work explains the design features of segmentally constructed bridges, with particular emphasis on the application of laboratory determined data in early age loading and high performance concrete.

AASHTO's LRFD [AASHTO, 1994] recommendations regarding the allowance of long-term effects in bridge design are reviewed. A practical procedure for extraction of actions due to creep, shrinkage and prestressing losses, for inclusion in AASHTO recommendations, is presented.

The structural modeling and the application of procedures are briefly illustrated through a numerical example of a prestressed precast spliced girder.

[1] Professor, San Francisco State University; Principal, ADAPT Corporation, 1733 Woodside Rd, #220, Redwood City, Ca 94061,e-mail: Support@AdaptSoft.com; web site: www.AdaptSoft.com

1 - INTRODUCTION

1.1 Segmental Construction

A segmentally constructed bridge is built from discrete components which are assembled over a period of time. In addition, a segmentally constructed bridge has one or more of the features described below:

(i) The components are called upon to carry loading in a configuration and through a construction-phase structural system other than that of the completed structure. A good example is balanced cantilever construction, where the cantilevering structural system of the bridge is for construction phase only.
(ii) The construction loading on the bridge components results in stresses which exceed those of the completed structure. Hence the design of the components, including the prestressing, is in part controlled by the construction technology. In many cable stayed bridges, the design of the deck depends on the construction equipment used, and is controlled through construction-phase support and loading conditions.
(iii) Early-age loading of concrete, oftentimes within the first 24 to 48 hours after casting, leads to high deformation values which must be carefully evaluated and accounted for deflection and camber control of the completed structure.
(iv) The bridge undergoes significant changes in its load carrying structural system during its erection. Spliced-precast-prestressed girder bridges are generally assembled with interim supports. As simply supported members they carry their selfweight. When spliced they take the load of freshly placed topping before the composite action sets in.
(v) The method of construction greatly influences the initial stresses in the completed structure to the extent that the analysis of the completed structure without regard to its construction scheme becomes irrelevant. Consider the span-by-span construction of a two span bridge made continuous over the common support. The selfweight moment at interior support is primarily governed by the method of construction.
(vi) Most retrofit projects involve addition of fresh concrete, external or internal prestressing, and recently developed synthetic fabrics (strips). Mixed material properties, the interaction of shrinkage and creep strains of the freshly placed concrete with the retrofitted components in resisting the applied loading, and the subsequent redistribution of loading among the new and existing components require time-delayed analysis specific to segmental construction.

In summary, where the effects of time, changes in the structural system, and high construction loads impact the performance and safety of a structure, during construction and when complete, there is need for a segmental construction analysis procedure [Aalami, 1993].

Prime examples of segmentally constructed bridges are:

- Prestressed-precast-spliced girders with post-tensioning and concrete topping
- Balanced cantilever construction
- Cable stayed bridges
- Various schemes of span-by-span construction for continuous bridge frames
- Incrementally launched bridges
- Bridges retrofitted with external tendons, concrete jackets, and synthetic fabrics
- Suspension bridges

1.2 Time Dependent Parameters

Time dependent concrete deformation is greatly amplified with early age concrete loading. Early loading, coupled with high construction stresses which may exceed service level conditions, bring to focal point the importance of deformation control in segmentally-constructed bridges. In concrete bridge construction, short and long-term control of stresses and deflections are customarily achieved through the application of prestressing and post tensioning tendons. **Creep, shrinkage**, and **aging** effects of concrete, as well as **relaxation** of prestressing steel, are the primary factors in the delayed displacement of a concrete structure. These time-dependent parameters are an essential consideration in the design and analysis of segmentally erected prestressed concrete bridges. Computational predictions will deviate significantly from the actual response of a prototype if the long-term effects are not realistically evaluated and allowed for in the analysis.

Creep is a stress originated effect and is dependent on, among other factors, the entire load history of the concrete element. Shrinkage is a non-stress originated factor. It is due primarily to reduction in water content and change in volume caused by carbonation. As concrete ages, its modulus of elasticity increases. Addition, or deletion of the same magnitude of loading at different ages results in different deformation in concrete. The impact of the creep component is by far the most complex to predict since it is a function of the entire load history of the structure.

Time dependency in prestressing is due entirely to the relaxation phenomenon similar in nature to the creep component of concrete. The relaxation of prestressing steel is defined as the decrease in tendon force with time under constant deformation.

Creep, shrinkage and aging of concrete and relaxation of prestressing steel may be classified as time dependent, material inherent parameters. The other class of time dependent parameters relates to construction scheduling and configuration of the structure. Segmentally-erected, prestressed concrete bridges often follow repetitive cycles of construction operations. The shorter is the cycle period, the younger is the concrete age at loading or prestressing, and the higher will be the concrete time dependent effects due to creep, shrinkage and aging. This, in turn, will lead to a higher degree of stress redistribution. Composite construction, consisting of casting new concrete against

aged components in segmental erection, adds to the complexity in prediction of the structural response.

Additional information on this topic may be found in [PCI, 1985, 1975, Tadros et al, 1975].

2 - REQUIREMENTS OF DESIGN TECHNOLOGY FOR SEGMENTAL CONSTRUCTION

Due to the special features of segmental construction, the design technology must have the following analytical capabilities.

(i) Ability to model the construction of the bridge as it is being installed. This includes addition of bridge components, and fasteners, and the addition or deletion of temporary member.
(ii) Capability to start the construction at several independent locations and at different times, each following its own schedule, and finally to bring the components into an integrated, completed structure.
(iii) Addition and deletion of temporary supports.
(iv) Externally applied displacements to control deformation
(v) Inclusion of the stiffness of construction equipment, such as launching girders and form travelers, when the attachment of the equipment to the bridge components affects the stiffness of the bridge structure
(vi) Capability to model both pre-. and post-tensioning, for bonded and unbonded construction and mixed systems
(vii) Capability to model external tendons
(viii) Capability to model cable stays
(ix) Full capability in modeling different concrete materials, based on model codes, or laboratory tests performed for the bridge under construction; ability to model as many material properties as the prototype calls for
(x) Authentic modeling of creep, and shrinkage
(xi) Allowance for aging of concrete
(xii) Determination of losses in prestressing due to friction, seating loss, stress relaxation, creep, shrinkage and aging of concrete

Apart from the essential features listed in the preceding, there are a number of convenience requirements, such as the ability to view the modeled structure and the computed solution. Graphical generation and display of both the structural model and the computed results greatly eliminates the potential for errors in data generation and interpretation of the results.

Other convenience features are the generation of AASHTO or other code stipulated combinations for code stipulated stress and strength checks, the generation of live loading, and the combination of solutions, and enveloping.

3 - AASHTO REQUIREMENTS

AASHTO is probably the only code in the international arena which stipulates requirements specific to segmental construction [AASHTO, 1989]. The requirements address stress and safety considerations during the construction, allowance for time-dependent effects, and the necessity to account for redistribution of stresses.

As an example, consider the case of a balanced cantilever construction shown in Fig. 3.1. The stresses at the tip of the approaching cantilevers are zero prior to closure of the spans. However, time dependent effects continue to act on the bridge after its completion and result in redistribution of the initial moments as illustrated in the schematic.

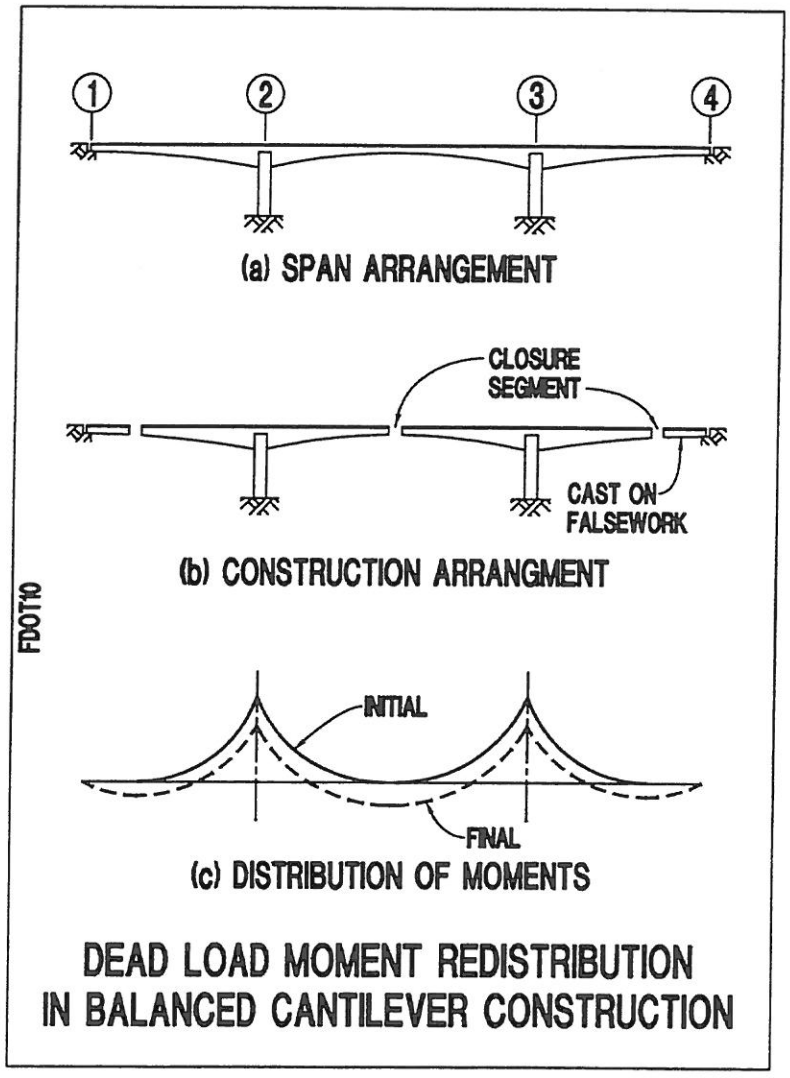

FIGURE 3.1-1

From a user's standpoint, compared to the alternative AASHTO [AASHTO, 1996] code, one difference of AASHTO LRFD [AASHTO, 1994] is the number and composition of load combinations for service and strength, and the associated load combination factors. The design procedure referred to herein [ADAPT, 1997] meets the requirements of segmental construction in accounting for the construction phase provisions, and the subsequent stress redistribution, and yields the load combinations necessary for AASHTO LRFD serviceability and strength checks. The formulation is general and can be applied directly to the specifications of other codes.

4 - CONCEPTUAL TREATMENT OF DESIGN PRARAMETERS

The following discourse reviews the design parameters of specific importance to segmental construction and their conceptual treatment in building codes and practice.

4.1 Aging of Concrete

Concrete gains strength as it ages. In addition, its immediate response to applied loading, expressed through its modulus of elasticity, changes, showing greater stiffness with lapse of time. The modulus of elasticity increases monolithically with time. As concrete ages, the rate of increase in strength decreases. The time-strength curve is assumed asymptotic to an upper bound value. The following describes the relationships used for the variation of concrete strength and modulus of elasticity with time.

4.1-1 Concrete Strength f'c

Concrete strength at any given day (t) is generally related to its strength at 28 days (f'_c). For normal weight and normal strength concrete the common relationships used are:

ACI-209 [ACI, 1992] recommends the cylinder strength $f'_c(t)$ to be computed using an equation of the form

$$f'_c(t) = [t/(a+bt)]f'_c(28) \qquad (4.1\text{-}1\text{-}1)$$

where

a, b = Constants as defined below
$f'_c(28)$ = Concrete strength at 28-day
t = Age of concrete in days past casting date

Constants "a" and "b" define the shape and the upper bound of the strength/time curve. The values of "a" and "b" depend on the type of cement and the curing method used for the specimen. The ranges of "a" and "b" for normal weight, sand lightweight, and lightweight concrete are: a=0.05 to 9.25 and b=0.67 to 0.98. For type I (common) cement and moist curing, the recommended values are a = 4.0 and b = 0.85.

CEB-FIP Model Code [CEB-FIP, 1990] expresses the development of concrete strength with time according to the following recommendation:

$$f'_c(t) = \exp\{s\,[1-(28/t)^{1/2}]\}\, f'_c(28) \qquad (4.1\text{-}1\text{-}2)$$

where

s = Coefficient as described below

The coefficient "s" depends on the type of cement: s=0.20 for rapid hardening high strength cements RS. 0.25 for normal and rapid hardening cements N and R, and 0.38 for slowing hardening cements SL.

For High Performance Concrete (HPC) the increase in strength is much faster than the code recommended relationships [Khan et al, 1997]. The code relationships quoted may not apply to HPC. For an accurate assessment, laboratory tests may become necessary.

4.1-2 Modulus of Elasticity $E_i(t)$

The development of modulus of elasticity of concrete with time is generally related to its strength at 28 days. For this reason, the expression for gain in strength with time assumes special importance, since it indirectly controls the displacement response of a structure under applied loading.

Using ACI [ACI, 1982] the time dependent elastic modulus $E_i(t)$ of concrete is computed as a function of the cylinder strength $f'_c(t)$.

$$E_i(t) = 33\, w^{1.5}[f'_c(t)]^{1/2} \qquad (4.1\text{-}2\text{-}1)$$

where

$E_i(t)$ = Modulus of elasticity in psi
f'c(t) = Concrete cylinder strength in psi on day, t
w = Unit weight of concrete in pounds per cubic foot

In SI units the relationship becomes:

$$E_i(t) = 0.043\, w^{1.5}[f'_c(t)]^{1/2} \qquad (4.1\text{-}2\text{-}2)$$

Where, w is in kg/m^3. The remainder of the parameters in MPa.

CEB-FIP [CEB-FIP, 1990] gives the modulus of elasticity of concrete at an age (t) other than 28 days with the following relationship.

$$E_i(t) = \{\exp\{s\,[1-(28/t)^{1/2}]\}\}^{1/2} * E_i(28) \qquad (4.1\text{-}2\text{-}3)$$

where

$E_i(28)$ = Modulus of elasticity in MPa at day 28
$E_i(t)$ = Modulus of elasticity in MPa at day, t
s = As given in Eqn. 4.1-1-3

4.2 Creep

Creep strain is defined as increase in strain under sustained stress with constant humidity and temperature. It is a stress originated strain. Creep strain does not include the instantaneous elastic deformation. Its rate decreases to zero over time and is only partially recoverable (see Fig. 4.2-1). Analytical estimate of structural response can be significantly in error if creep effects are disregarded. Creep is generally responsible for large deformations and significant redistribution of stress.

Creep strain at any time under constant stress is computed using one of the several available empirical relationships. The relationships express the creep strain on day (t) as a fraction of the "ultimate creep coefficient" C_u. The ultimate creep coefficient is the maximum creep attained at time infinity for a lab specimen under controlled and constant conditions. In the prediction models, only those parameters are taken into account which are normally known to the designer, such as characteristic compressive strength, dimensions of member, mean relative humidity, age at loading, and duration of loading. Due to dependency of creep on other factors which are not accounted for in prediction formulas, and the errors in the determination of the parameters described, discrepancies up to 20% between the computed and observed creep values are not uncommon..

ACI [ACI, 1982] makes the following recommendation:

$$\varepsilon_c(t) = K_S * K_H * K_h * K_\tau * \{(t - t_o)^{0.6}/[10 + (t - t_o)^{0.6}]\} * C_u \qquad (4.2\text{-}1)$$

where,

t = observation time in days
t_o = age at loading in days
$\varepsilon_c(t)$ = Creep coefficient = (creep strain at time t)/(initial immediate strain)
C_u = ultimate creep coefficient determined by experiment for specimen loaded at age of 7 days
K_S ,K_H ,K_h ,K_τ are coefficients accounting for the slump of mix, humidity, member thickness and age of loading. [ACI 1982]

Creep of high strength concrete is much more sensitive to the age of loading than that of the normal and medium-strength concrete, with very early-age loading resulting in significantly higher creep [Khan et al, 1997]

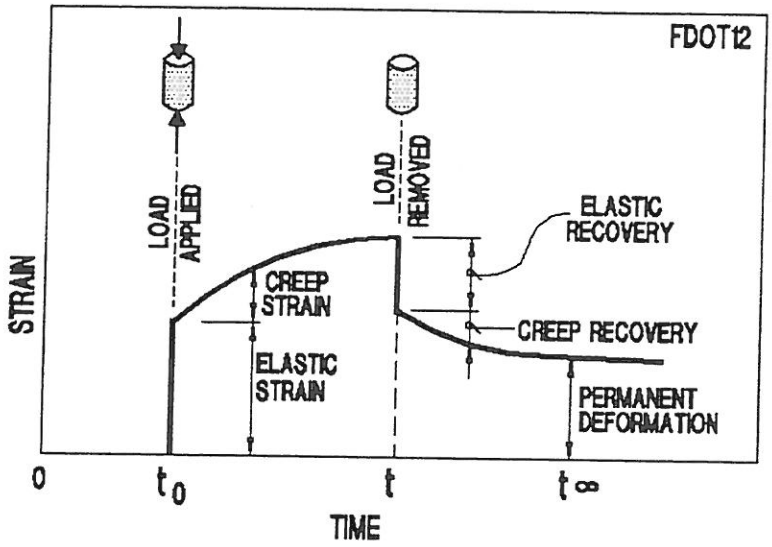

CREEP RESPONSE OF CONCRETE

FIGURE 4.2-1

For normal strength concrete, the ultimate creep coefficient, C_u varies between 1.50 and 3.00. None of the relationships described are intended to describe the response of high performance concrete. For HPC specific lab tests are recommended.

4.3 Shrinkage

Shrinkage strain, $\varepsilon_s(t)$, is a non-stress originated strain defined as the deformation under neither load nor temperature change. Shrinkage of concrete is primarily due to loss of water upon drying (drying shrinkage) and volume change due to carbonation (carbonation shrinkage). Shrinkage rate decreases to zero over time (see Fig. 4.3-1). In most structures, shrinkage strain is greater than strain due to applied loading. Its allowance in the analysis becomes critical for the computation of stresses and deformations.

ACI [ACI, 1982] recommends the following relationship for shrinkage computations:

$$\varepsilon_s(t) = K_S * K_H * K_h \{(t - t_o)^e/[f + (t - t_o)^e]\} * S_u \qquad (4.3\text{-}1)$$

where,

$\varepsilon_s(t)$ = shrinkage strain at observation time, t
S_u = ultimate shrinkage strain determined by experiment
t = observation time in days
t_o = age of curing in days
f, e = constants, determined from experiments [ACI 1982]
K_S , K_H , K_h = slump, member size and relative humidity correction factors [ACI 1982]

The constant "f" varies between 20 and 130. For normal strength, normal weight concrete, f, is assumed 50. Similarly, the constant "e" varies between 0.9 and 1.9. For normal conditions, e is assumed equal to 1.

The ultimate shrinkage coefficient for most structures varies between 400 and 1000 ms

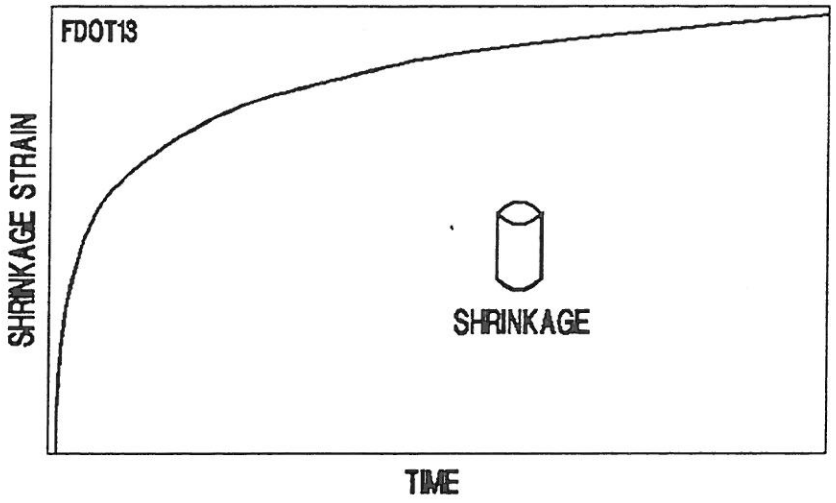

VARIATION OF SHRINKAGE STRAIN WITH TIME

FIGURE 4.3-1

4.4 Loss of Stress in Prestressing

4.4.1 Relaxation in Prestressing

Prestressing tendons lose a fraction of their initial stress with time due to a phenomenon called "relaxation." Relaxation is similar in nature to the creep of concrete. The relaxation of prestressing steel is defined as the decrease in tendon force with time under constant strain. Most commercially available prestressing steel is classified as either low relaxation or stress relieved. Low relaxation prestressing steel experiences less reduction in force with time compared to its stress relieved counterpart.

The prestressing steel is treated as a linear elastic material subject to time dependent strains of relaxation. The following equation [Magura et al, 1964] is generally used for the calculation of tendon stress due to relaxation under constant strain.

$$f_s = \{1.0 - [(\log t)/c]*[(f_{si} / f_{sy}) - 0.55]\}*f_{sy} \qquad (4.4.1\text{-}1)$$

where,

f_s = steel stress at time t

f_{si} = initial steel stress

f_{sy} = 0.001 offset yield stress

c = constant (= 10 for stress relieved strand; = 45 for low relaxation strand)

t = time in hours after stressing

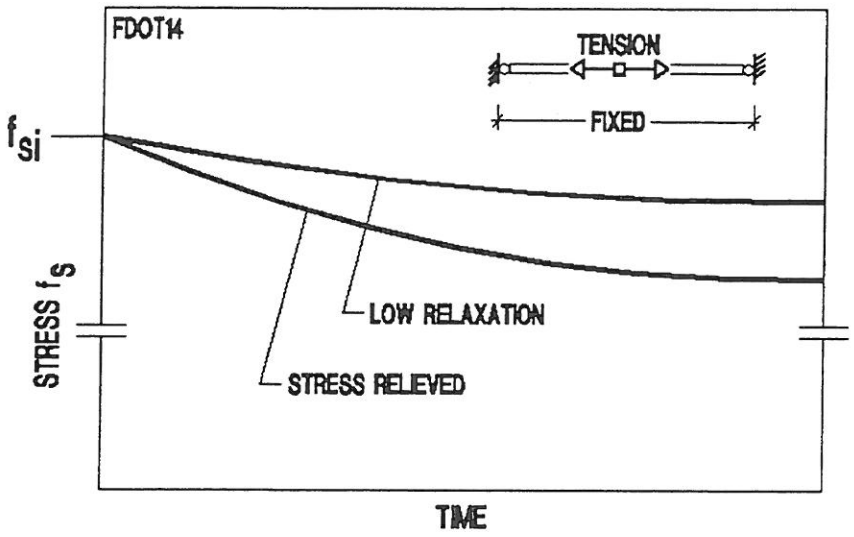

STRESS LOSS IN PRESTRESSING
DUE TO RELAXATION

FIGURE 4.4-1

4.4.2 Stress Loss in Prestressing Due to Other Time-Dependent Parameters

The state of stress in a prestressing steel is indirectly affected by other time dependent parameters, such as creep, shrinkage and aging of concrete. Further, variations in concrete strain due to applied loading and/or temperature also result in changes in tendon stress, and consequently impact the deformations and stresses in the structure. There will be a redistribution in prestressing force, generally larger in magnitude than the loss due to relaxation, from the indirect factors enumerated. While the indirect loss in prestressing and the necessity of its allowance in the computations are recognized in the design codes, there are no specific procedural recommendations for their evaluation. Several approximate procedures are common among design engineers [PCI , 1985]. This work includes the outline of an approach tailored to segmental construction.

4.5 Construction Time and Sequence Schedules

Sequence of construction, construction equipment used, and the time-schedule of an incrementally constructed bridge have significant impact on the long-term performance of

a bridge. Consider the case of the incrementally launched bridge illustrated in Fig. 4.5-1. Segments, typically one half the span are cast against a former segment on a fixed bed on one embankment. The cast segment is then stressed and pushed forward with the remainder of the bridge to cover the spans. The stresses and deformations during the construction, and immediately at completion of construction, are primarily governed by the sequence and time-table of construction. When complete, the construction stresses locked in the bridge deck impact the long-term deformation and stresses of the bridge in service.

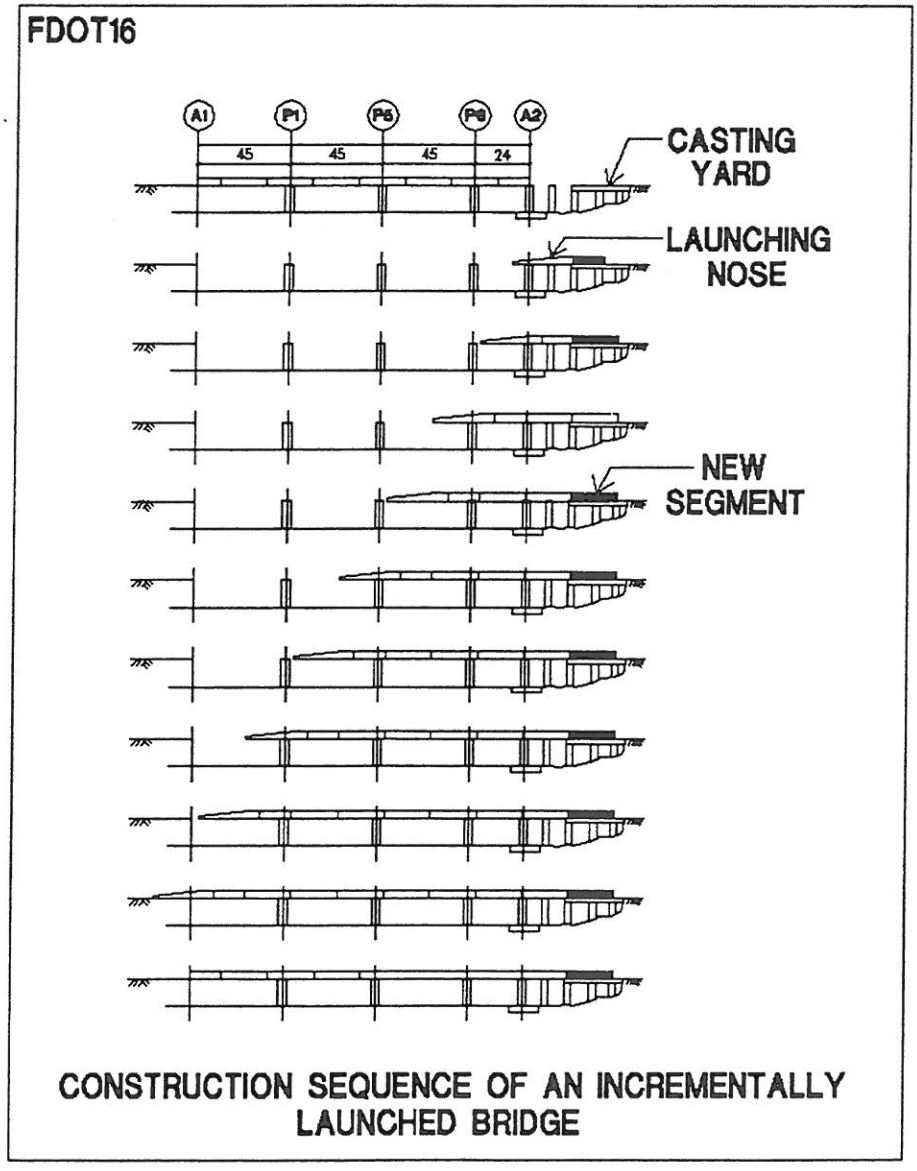

FIGURE 4.5-1

4.6 Temperature

Temperature induced stresses are not time-dependent items in the same sense that creep, shrinkage, stress relaxation and aging of concrete are. With respect to their occurrence, temperature stresses are more akin to those induced by live loading (vehicular loading). However, since in the load combinations stipulated in AASHTO LRFD [AASHTO, 1994] temperature induced stresses are grouped with creep and shrinkage, the treatment of temperature loading is handled at the same instance as the time-dependent parameters.

AASHTO stipulates two cases of temperature loading. One loading is due to the direct and daily radiation of the sun, causing a sharp temperature gradient through the depth of the bridge. The other is due to seasonal changes in temperature and results in a somewhat uniform change in temperature through the depth of the bridge section over a longer period of time.

The applicability of AASHTO recommended temperature stresses to practical design is subject to controversy. The computed stresses from AASHTO induced temperature gradient do not appear to conform with the observed response of structures in all instances. Temperature stresses are not expounded in this work.

4.7 Settlement of Supports

Settlement of supports is gradual. Creep in concrete reduces the impact of settlement induced stresses. In the analysis of segmentally constructed bridges, settlement must be applied in steps over time, in order to capture the softening effect of creep in concrete.

AASHTO LRFD [AASHTO, 1994] groups the stresses induced due to settlement with the other time-dependent parameters creep and shrinkage.

5 - PRACTICAL IMPLEMENTATION OF DESIGN PARAMETERS

5.1 Determination of Design Parameters

5.1-1Code Models and Recommendations

A - Characteristic Values (f'_c, C_u, S_u)

For convenience in practical design, the response of structural concrete to instantaneous and long-term effects is, by convention, described in terms of characteristic values obtained through laboratory controlled standard tests. When applied to a prototype, the characteristic values obtained in the laboratory are adjusted through coefficients which represent the deviation of the prototype from the laboratory conditions under which tests for the characteristic values were performed.

The most common characteristic value is the compressive strength of concrete at 28 days, measured either using a standard cylinder (f'_c), or a standard cube (f'_{cu}). As a first approximation, for normal weight and normal strength concrete, the cylinder strength is assumed to be 80% of cube strength of the same material.

For shrinkage, the ultimate shrinkage coefficient (S_u) is defined as the maximum shrinkage strain attained at time infinity for a lab specimen under controlled conditions.

The ultimate creep coefficient (C_u) is defined as the maximum strain per unit of applied stress, attained at time infinity in a lab specimen, when the specimen is loaded at a specific age and retained constant stress thereafter for the entire duration of the test. ACI [ACI, 1992] expresses C_u for the specimen loaded at age 7 days. The CEB code [CEB, 1990] defines C_u for loading at age 28 days. Obviously, for the same specimen the two values will be different. As a first approximation, and for normal concrete, the ultimate shrinkage coefficient determined using ACI would be 40% higher than the associated value from CEB.

Since it is not practical to have an experimentally obtained ultimate creep and shrinkage coefficient (C_u and S_u) for most bridge prototypes, building codes propose empirical relationships to estimate C_u and S_u. The relationships are based on the composition of the concrete mix. A more frequently used alternative, is to select values which have been derived from the observed deformation performance of similar construction. For example, for free cantilever construction, the measured deformation at the tip of the segments being constructed is correlated to the computations by adjusting the assumed characteristic values C_u and S_u. The adjusted values are used to predict the deformation of subsequent construction.

B - Variation of Creep and Shrinkage Strain With Time

Refer to Fig. 5.1-1(a). Point A represents the ultimate creep or shrinkage strain attainable for a given specimen. The deformation of a prototype, particularly in segmentally constructed bridges, is governed by the manner in which the creep or shrinkage builds up over time. For illustration purposes, the figure shows three paths marked 1, 2 and 3 in reaching the ultimate value, A. Apart from the recommendations for the estimate of the ultimate creep and shrinkage coefficients (point A), each of the two codes (ACI and CEB) suggest expressions for the shape of the creep and shrinkage curves, such as illustrated by curves marked 1,2 and 3. The ultimate coefficient and the shape function enable the designer to estimate the values of creep and shrinkage at different times.

One method of treatment of the creep and shrinkage curves, such as the samples shown schematically in part (b) of Fig. 5.1-1, is to normalize the curves with respect to the ultimate value (A) as illustrated in part (a) of the figure. When normalized, the analysis proceeds with the value of the ultimate coefficient (A) and a shape

function describing the characteristics of the curve. Adjustments between the computed and observed values are implemented by changing the value of the ultimate coefficient only (point A).

C - Scaling of creep and shrinkage curves

An alternative shown in part (c) of Fig. 5.1-1 is to select a curve which is proven to yield acceptable results for a class of construction, and scale its values in applying it to a particular project. This alternative is practiced when a particular code, proven to be successful in one locality, is adopted for application to similar structures in other parts of the world and yields consistent under-. or over estimate of deformations for time-dependent effects. An example is concrete structures built in Hong Kong, where actual structures consistently exhibit a larger long-term deformation than those in Britain when using the British code. In this case, a scaled version of the code- generated curve can be used. The scaling retains the shape of the code-derived curve, but increases or decreases its value by a given scale along the length of the curve.

5.1.2 Laboratory Models

A - Material Tests, Test Results and Their Interpretation

(i) Shrinkage

Shrinkage response is obtained through laboratory testing of specimens built to specifications (Fig 5.1-2a) and kept under controlled environmental conditions. For specimens from a prototype, readings are normally made for observation times extending 30 to 60 days. Extrapolation of these readings becomes necessary to determine shrinkage response beyond the time range of the lab specimens. While a general purpose best fit curve can be used to represent the lab readings and afford extrapolation, code suggested expressions, such as the expression 5.1.2-1 derived from 4.3-1 are more suitable.

$$\varepsilon_s(t) = K\{(t - t_o)^e/[f + (t - t_o)^e]\} * S_u \qquad (5.1.2\text{-}1)$$

Where, K, represents the product of coefficients from 4.3-1 specific to the lab specimen being tested.

Using code recommended values of , e, and, f., and laboratory readings, an average ultimate shrinkage coefficient is estimated. In Fig. 5.1-2, the extrapolation beyond the last lab reading is shown by broken lines. Shrinkage values for days falling within the extrapolated region are determined using the extrapolation curve. Finally, a table consisting of days and their associated observed, or extrapolated shrinkage strains is generated and used as entry data for bridge analysis.

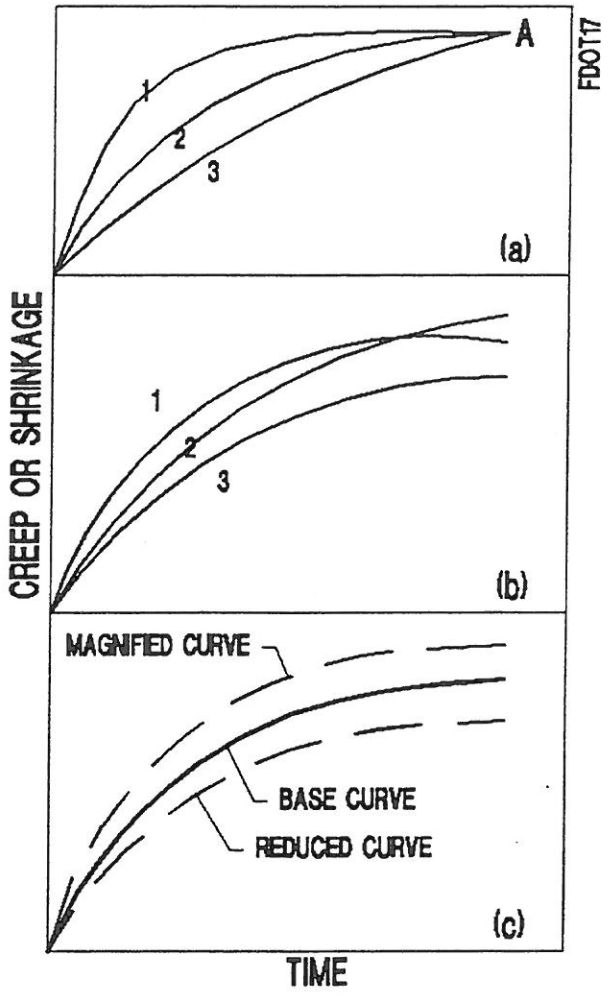

TREATMENT OF CREEP AND SHRINKAGE CURVES IN DESIGN

FIGURE 5.1-1

(ii) Creep

In using laboratory generated values to investigate the creep response of a structure three measurements are sought. These are: (a) the specimen's instantaneous response to the applied loading, referred to as elastic response; (b) creep deformation of the specimen with time; and (c) the ultimate deformation of the specimen.

Unlike shrinkage, where one specimen from each concrete mix can be adequate to generate data for the shrinkage response of the prototype, for creep analysis the number of lab tests depends on the number of principal loading applications of the prototype. This is expounded in more detail next.

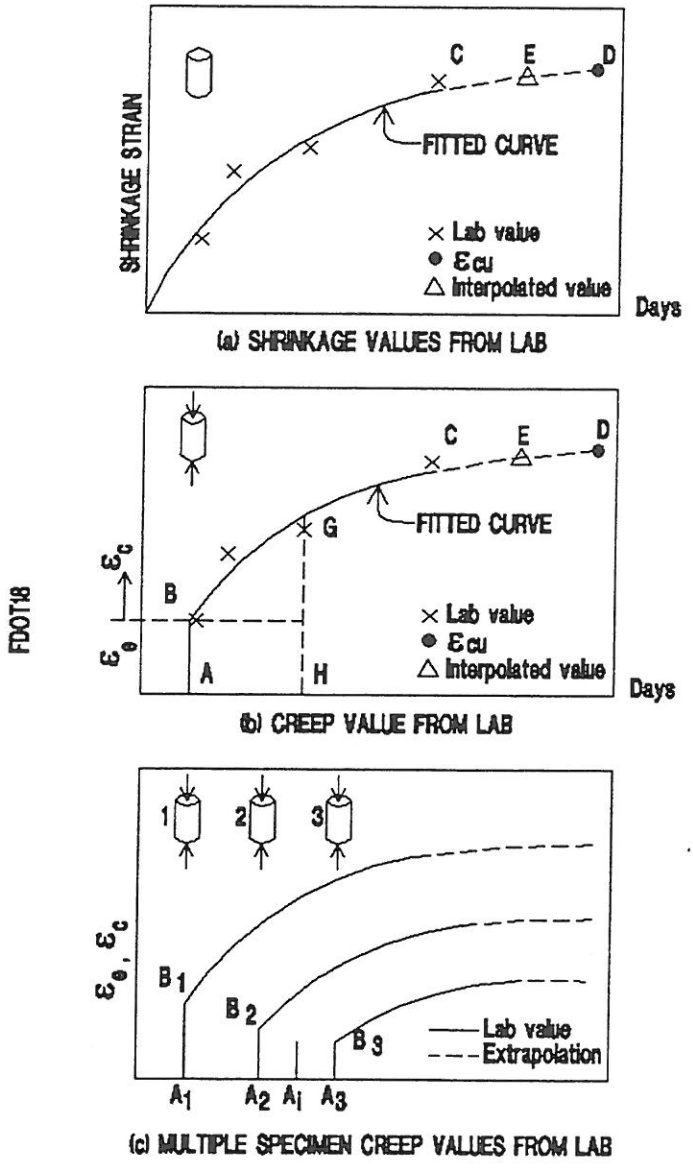

FIGURE 5.1-2

Single Loading Case

The simple case involves the response of a structure to a single and instantaneous application of loading. An example of this case is the creep response of a cast in place box girder bridge (Fig. 5.1-3) after the removal of shoring. The impact of selfweight activated at time of removal of shoring is the one-time principal loading responsible for the creep of the structure. For this condition, a single lab test as illustrated in Fig. 5.1.2(b) would be adequate, provided the time of loading of the lab specimen (point A) matches the day of removal of shoring in the prototype.

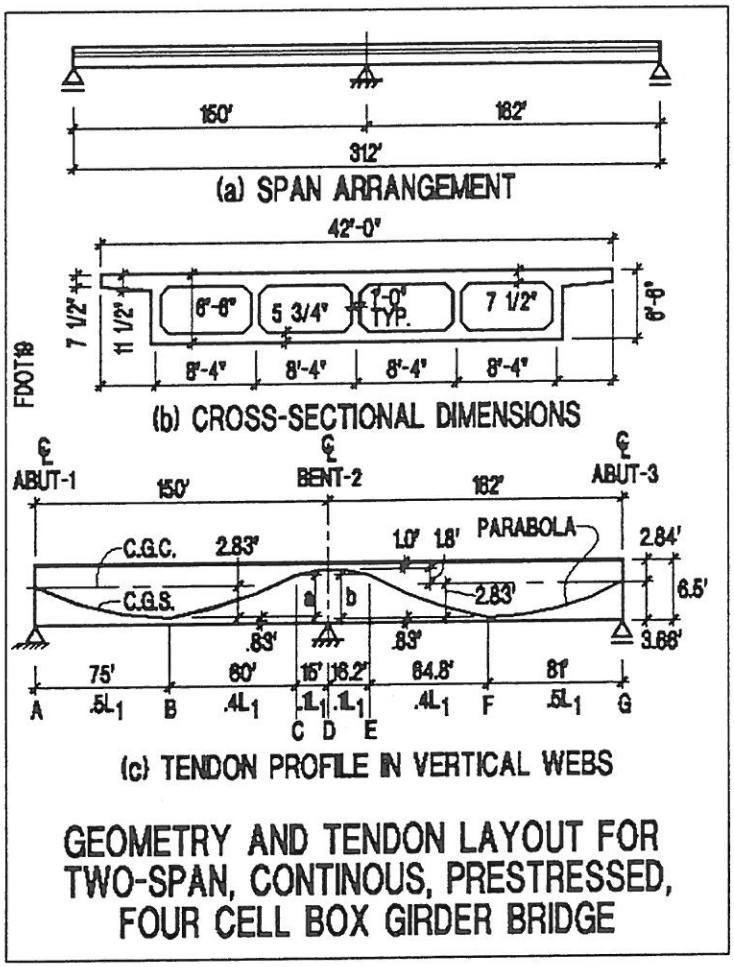

FIGURE 5.1-3

A creep lab test aimed at generating data for the response analysis of a specific prototype includes the following.

(a) A concrete specimen (such as a standard cylinder) must be made from the same mix as the prototype. This specimen must be kept under the same environmental conditions (temperature, humidity) as the prototype. Typically, the specimen is stored next to the prototype.

(b) Since the creep response of concrete depends on the age of concrete at the time the loading is applied, the loading age of the specimen and the prototype must match. The magnitude of the applied loading on the lab specimen, however, is not critical, since the creep strain is assumed to be proportional to the applied stress, and is expressed in terms of strain per unit stress. Line AB is Fig. 5.1-2b indicates the instantaneous shortening of the test cylinder. From the instantaneous shortening, using Hook's Law in uniaxial loading, the modulus of elasticity at the time of loading is calculated.

(c) The loaded test specimen is kept under the same environmental condition as the prototype. From time to time, such as at days 1, 3, 5, 7, 14, 28, the shortening of the

test specimen is measured. From the shortening, the creep strain for each of the observed days is calculated. The creep strain divided by the applied stress on the specimen is used as entry data for the analysis of the prototype. As an example, for the observed day H, shown in Fig. 5.1-2(b), the total strain is shown by the ordinate of point G. The creep strain to be used in the creep computations is the difference between the ordinates of points G and B.

(d) If the last observed lab measurement is point C on the chart, but it is intended to estimate the response of the structure at a later date (point D on the chart), a curve is approximated through the measured points B through C. The approximated curve is extrapolated to give the estimated ultimate creep coefficient (D). The following relationship is generally used to obtain an approximate curve, fit to the measured creep strains

$$C(t) = K_s * K_H * K_h * K_\tau * \{(t - \tau)^{0.6}/[10 + (t - \tau)^{0.6}]\} * Cu \qquad (5.1.2\text{-}2)$$

where,

t = observation time in days
τ = age at loading in days
$C(t)$ = Creep coefficient = (creep strain at time t)/(initial immediate strain)
C_u = ultimate creep coefficient determined by experiment
= 2.35 for standard conditions
K_s ,K_H ,K_h ,K_τ are coefficients accounting for the slump of mix, humidity, member thickness and age of loading. [ACI 1982]

Should values between the last laboratory reading (point C) and the assumed limit of the extrapolation day (point D) become necessary, the relationship for the approximated curve is used to generate assumed observation values such as point E in Fig. 3.1-2b.

Multiple Loading Case

Multiple test specimens are required, when the principal long-term loading on a structure is not applied at one time. Consider the case of a precast prestressed I-girder bridge with a topping slab, such as the schematic of Fig. 6.1-1. For creep computations, the load due to the weight of the topping is considered to have been applied instantaneously and remains on the precast prestressed girder indefinitely. There will be no other major application of dead load to the bridge subsequent to the placement of the topping.

A different scenario is the case of a segmentally constructed free cantilever bridge. Addition of each new segments, adds a significant value to the loading of a previously installed segment. The loading of each segment is thus introduced in steps and at different time intervals. Fig. 5.1-2c illustrates the data necessary for the computation of creep response of such structures. The following describes the procedure.

(a) Several test cylinders from each segment of the bridge are cast and maintained in the same environmental condition as the prototype segment. In Fig. 5.1-2c, it is envisaged that the segment under consideration will receive three significant loads applied at days marked A1, A2 and A3 in the figure.

(b) In concert with the loading of the prototype, or as closely as practical, the test specimens are loaded. Each specimen is kept under observation and its creep strain measured and recorded. The outcome of the observation will be a chart containing: moduli of elasticity associated with each of the three loading times; and a table of observation days and associated creep values for each of the three specimen

Similar to the single case loading, the observed lab measurements can be extrapolated to generate data for prediction of the structure response beyond the last day of observation (shown in broken line in the figure).

In most prototypes, such as a free cantilever bridge, the creep response of a segment must be estimated before the segment is installed. Adjustments to vertical alignment (camber adjustment) are effected at the time of installation of segments. In such cases, the following procedure may be followed. First, prior to installing a segment, specimens of the same mix as projected for the segment to be placed are cast, tested in the lab, and their observed response used to predict the creep of the prototype. Second, specimens from the actual segment are used to verify the validity of the first group. Should the two results be significantly different, a re-analysis is performed for the bridge under construction. Necessary adjustments to the predicted camber calculation are introduced on the alignment of subsequent segments. It is not uncommon to implement corrections in the alignment of subsequent segments, based on the measurements of installed segments.

Construction cycles often differ from the predicted schedule. A set of laboratory observations geared to specific loading dates, such as shown in Fig. 5.1-2c (days A1, A2, and A3) may not match the loading ages of the prototype. The modification is achieved through linear interpolation between the approximated curves of the available observation dates.

(iii) Relaxation Tests

Almost all prestressing wires come with the manufacturer's data on relaxation. For any given prestressing material, the loss in prestressing depends primarily on the initial stress of the loaded strand wire. The stress losses can vary by several times, depending on the metallurgical composition and the manufacturing process of the strand wire.

To obtain the relaxation characteristics of a wire, the wire is stretched to a given strain and locked in position. With constant temperature and fixed initial strain, the loss of force in the wire is measured after a given time (typically 1000 hours)

Results of relaxation test are reported similar to the Table 5.1.2-1.

TABLE 5.1.2-1 EXAMPLE OF A TYPICAL RELAXATION TEST RESULTS

Wire	Ratio of initial to breaking stress	Loss in stress (%)	Hours
1	0.80	12	1000
2	0.70	8	1000
3	0.60	4.5	1000

The relaxation coefficient, c, may be computed from the following expression, derived from the relationship (Eqn. 4.4.1-1) with rearrangement of terms. Table 5.1.2-1 contains all the parameters of the right-hand-side.

$$c = [\log(t)/(1-f_s/f_{si})]^* [1.053(f_{si}/f_{pu})-0.55] \qquad (5.1.2\text{-}2)$$

The coefficient, c, obtained from the preceding is then used in the expression 4.4.1-1 to predict stress losses at times other than the lab measurements.

5.2 Implementation of Design Parameters

5.2.1 Creep Implementation - Stress History

Among the time dependent parameters of concrete, only creep effects are function of the entire stress history of the structure (Fig. 5.2-1(a)). An efficient solution protocol for the prediction of creep strains covering the entire stress history has been developed [Mokaddam, 1969, Kabir, 1976], and successfully implemented by previous investigators [Kang and Scordelis,1980]. This method, which is now the preferred procedure for modeling the creep response under multiple loading conditions is based on the principle of superposition, illustrated schematically in Fig. 5.2-1(b). Further, it is assumed that the creep component is a linear function in stress. The components of the superposition are creep curves from single loading condition, such as shown in Fig. 4.2-1 and Fig. 5.1-2.

5.2.2 - Relaxation in prestressing - Stress History

In a prototype, strain in prestressing strands are not constant. Creep, shrinkage and external loads cause additional changes in strain over time. To incorporate these additional force variations over time, the computation of stress in strand is made subject to an applied strain history [Hernandez and Gamble, 1975]. The procedure is further simplified by assuming that all non-relaxation changes in tendon force occur at the ends of the time steps.

Refer to Fig. 5.2-2. At time t_1, externally caused strain changes cause the tendon force to change to f_{s1}. To compute the stress relaxation δf_{r2} during the time interval δt_2, (time lapse between days t2, and t1), Eqn. 4.4.1.1 is used to calculate a fictitious initial tendon force f_{si1} which would have relaxed by δf_{r1} to f_{s1} during δt_1, (time lapse between t_1 and t_o. The stress f'_{s2} may then be found, assuming f_{si1} as the initial tendon force and Eqn. 4.4.1.1. This procedure is applied to each tendon segment during each time step to arrive at the total stress relaxation at time t_n. It assumes that the impact of creep, shrinkage and any other strain is takes place instantaneously at times t1, t2, .. ti. The accuracy of the solution is enhanced by selection of shorter time intervals.

5.2.3 Aggregated Stress Losses in Prestressing

Many approximate methods have been in use for the computation of the sum of stress losses in prestressing tendons [PCI, 1985] encompassing the contribution of all other factors. The approximations are necessitated due to shortcomings in the modeling of tendons using the equivalent load method. New analytical modeling techniques [ADAPT manual, 1996] eliminate the complexity of stress loss computations and the necessity of approximations inherent in the equivalent force method. The analytical modeling of prestressing tendons using both schemes are described next.

(i) Tendon Modeling Using Equivalent Force Method

Consider the partial elevation of a post-tensioned member shown in Fig. 5.2-3. The tendon can be envisaged to consist of a number of straight segments along the length of the original profile (Fig. 5.2-3(b)). The forces exerted by the tendon on the concrete at the vertices of the discretized tendon segments are transferred to the centroid of concrete member (Fig. 5.2-4). These forces, which are referred to as equivalent tendon force, are derived from the tendon force at stressing. Generally, they include the immediate losses in stress due to friction and seating of tendons. Since in this modeling scheme there is no coupling between the initially computed tendon forces and the subsequent response of the structure, such as the impact of shrinkage, the losses in prestressing must be implemented through approximated indirect schemes.

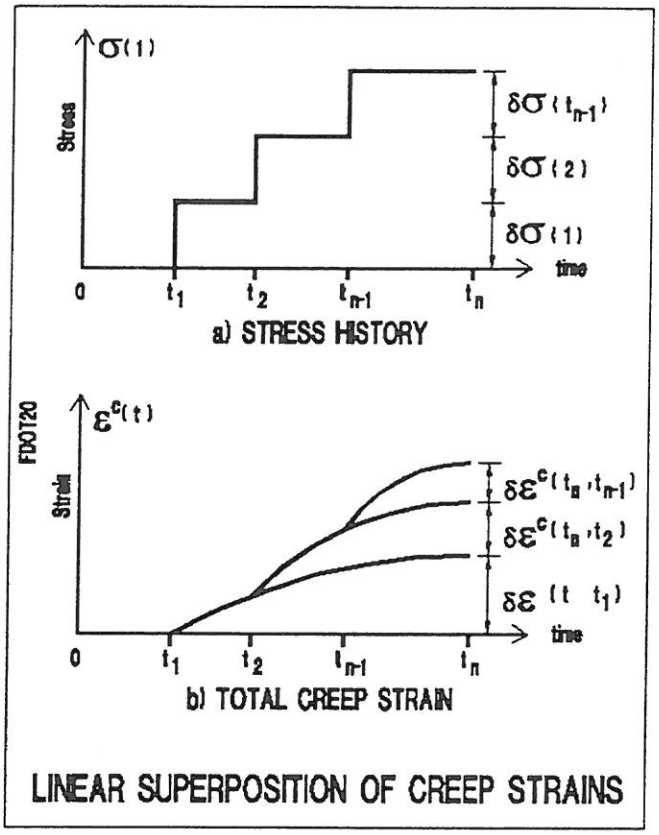

FIGURE 5.2-1

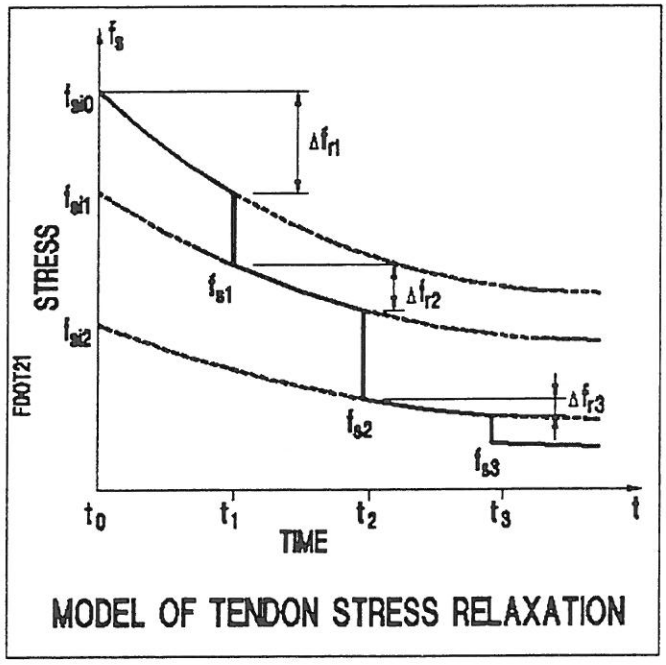

FIGURE 5.2-2

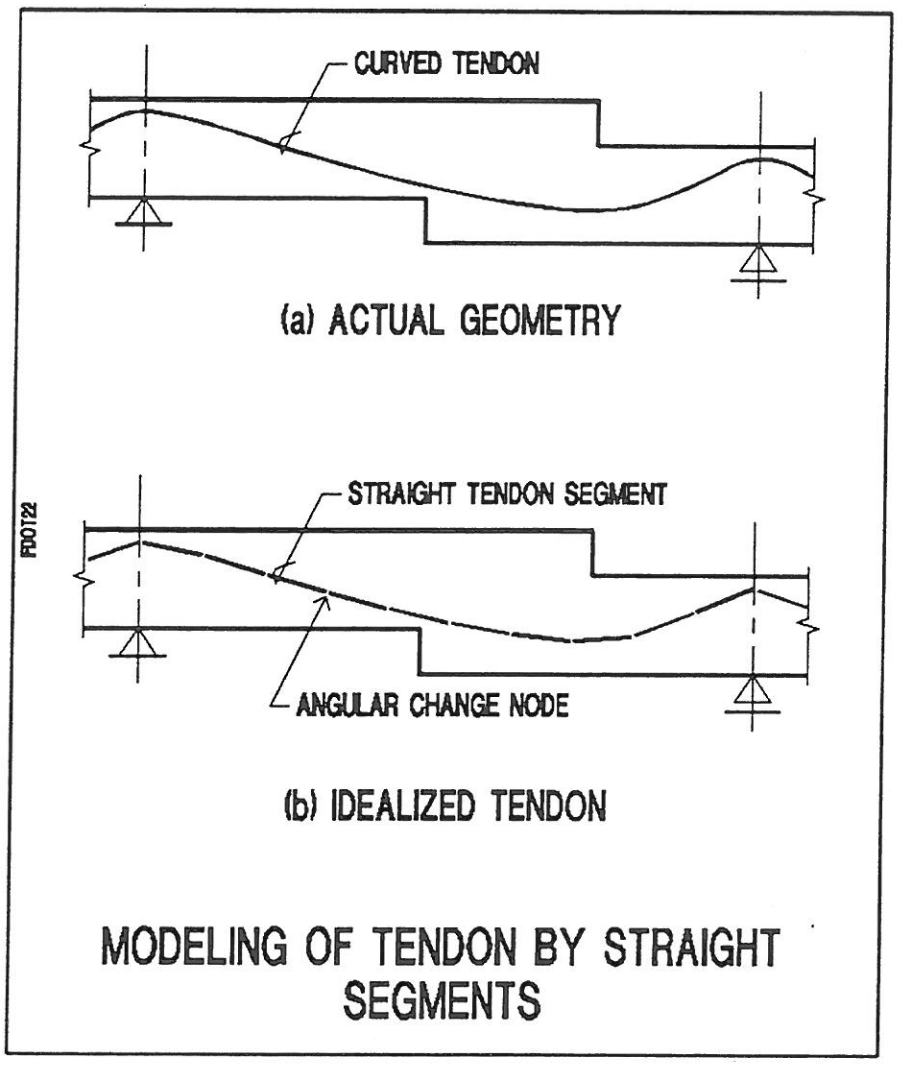

FIGURE 5.2-3

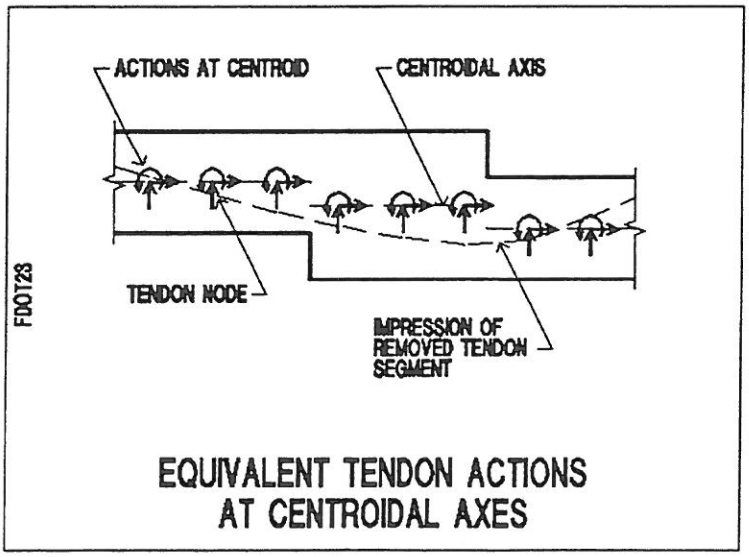

FIGURE 5.2-4

(ii) Tendon Modeling Using Discrete Elements

A major breakthrough in modeling of tendons and the direct integration of stress losses into the analysis is modeling of tendons as discrete finite elements, similar to the concrete segments. This method allows the tendon to experience the deformation of the structure within which it is housed, and to which it is bonded. The deformations due to time-dependent factors, such as creep, as it occurs, and when it occurs, will faithfully impact the tendon force. This procedure eliminates the question of stress loss computation as an independent operation.

Fig 5.2-5(a) illustrates a concrete segment from a prototype represented as a finite element, together with a segment from a tendon associated with it. The ends of the tendon segment are shown offset from the face of concrete segment, in order to covey the generality of the approach. The ends of the tendon segment (marked as tendon nodes) and the frame nodes (centroidal points at ends of concrete segment) are assumed to be rigidly connected (Fig. 5.2-5(b)). The tendon segment is modeled as a truss element. Consequently, change in tendon force in the segment shown becomes a linear function of the change in distance between its two ends (tendon nodes).

Using the assumption of plane sections remaining plane, and the rigid constraint between each tendon node and its associated frame node, the length of tendon segment and its associated force is directly coupled to the deformation of the concrete segment. Thus, deformations in concrete due to creep, shrinkage, aging strain, temperature, and applied loading are all imparted to the tendon through the tendon segment's immediate elastic and long-term relaxation characteristics. Likewise, through imposition of static equilibrium at each element face, a change in tendon force will affect the actions on the concrete section. Using this approach, long-term stress losses and the interaction between tendons and concrete become implicit in the modeling. Consequently, it will no longer be necessary to perform long-term stress loss computations.

5.3 Extraction of Actions and Displacements Due to Time Dependent Parameters

Time dependent factors, when present, influence the behavior of a prestressed member. For creep and prestressing force in tendons, the degree and manner of impact depends on the presence and nature of other time-dependent parameters, such as shrinkage. By convention and practice, as opposed to the rationale of structural performance, AASHTO, as well as several other design codes require that the impact of each of the time dependent parameters on the performance of the structure be evaluated independently, and be included in the design, each with its own load factor.

Ideally, selfweight, prestressing, creep and shrinkage should be lumped together producing a single response to be combined with other items, such as live loading for serviceability and strength checks. Uncertainties in estimating the characteristic values of

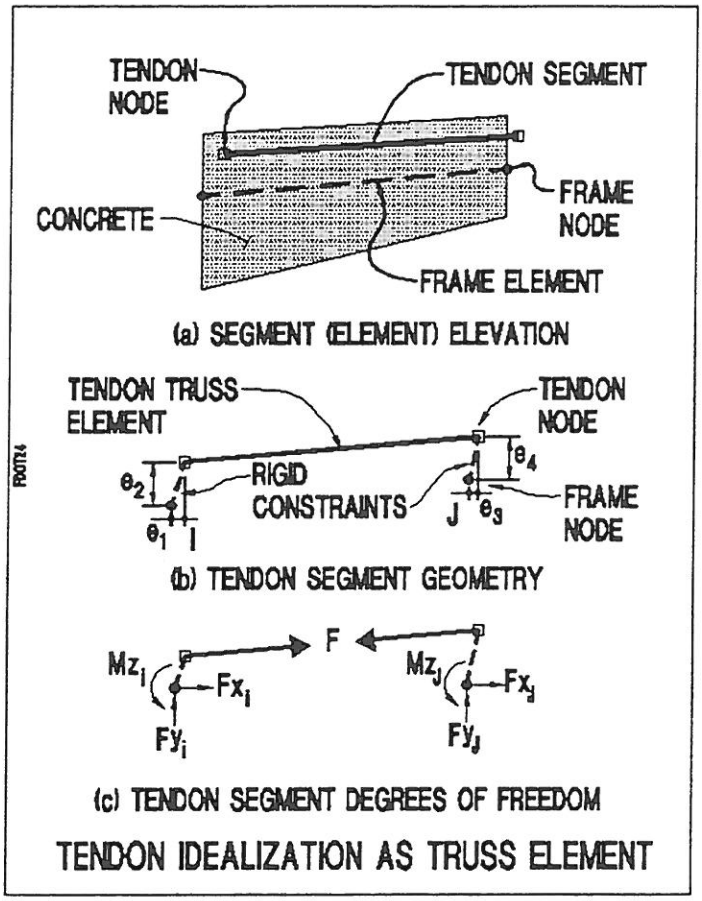

FIGURE 5.2-5

creep and shrinkage can be implemented by the introduction of lower and upper bound limits, and performing two sets of computations, one representing each of the extremes .

An authentic analysis must be based on an integrated solution allowing full interaction of all of the time-dependent components. To retain the authenticity of the analysis, and at the same time to comply with AASHTO [AASHTO, 1994] requirements, it becomes necessary to develop a post-solution analysis aimed at extraction of the solution components. The following describes the basis of the approach.

For any time interval there will be a change in deformation of the structure, δu, from which the change in stress will be computed. The change in deformation of the structure (δu) is caused by a combination of factors, which for simplicity are referred to as change in loading (δp). The relationship is:

$$[A]\{\delta u\} = \{\delta p\} \qquad (5.3\text{-}1)$$

[A] is the stiffness matrix of the structure. It is set up at the beginning of the time interval from the configuration and boundary conditions of the structure, at the construction stage, and at the time the solution is being sought. The stiffness matrix is based on the modulus of elasticity of each of the concrete components at the time of the solution, thus allowing

for aging of concrete to take place. The stiffness matrix [A] also includes the stiffness of the construction equipment, such as form travelers, if these equipment significantly affect the stiffness of the bridge under construction.

The loading increment $\{\delta p\}$ consists of the following components, all of which are either first introduced, or relate strictly to the time interval under consideration.

$$\{\delta p\} = \{\delta F + \delta T + \delta Cr + \delta Sh + \delta PT + \delta PTloss + \delta D\} \qquad (5.3\text{-}2)$$

where,

δF = increment of externally applied loading
δT = increment of temperature over the time interval
δCr = increment of loading on the structure associated with creep strain
δSh = increment of loading on the structure associated with shrinkage strain
δPT = increment of applied prestressing over the time interval
$\delta PTloss$= loss in prestressing force during the time interval
δD = increment of applied displacement to the structure over the time interval, including the settlement of supports

The creep component, δCr, is due to the action of stresses in the structure during the time interval being solved. Since the stresses are not known at the beginning of the time interval, the magnitude of δCr is not known a-priori. The loss in prestressing forces, $\delta PTloss$ - more appropriately termed "change in prestressing force" - apart from relaxation of strands during the time interval, depends on the shrinkage, creep, and the displacement response of the structure to other loading. The solution, therefore, becomes iterative. The iteration is pursued until equilibrium is achieved and the change between successive iterations reduces to less than a pre-defined accuracy [ADAPT, 1997].

In addition to its iterative nature at any time interval, the will be incremental to represent the progress of construction.

For completeness, note that at the end of each time interval, due to aging of concrete over the time interval, the stiffness of the structure represented by [A] is slightly changed. In the analysis referred to herein, the impact of this change in stiffness is lumped with the creep component of the next time interval.

Once, at the end of a time interval a solution is completed, the values of the constituents of the loading increment $\{\delta p\}$ are all known. The loading increment $\{\delta p\}$consists of constants and time and/or stress dependent components as indicated below.

$$\{\delta p\} = \{\delta F + \delta T + \delta PT + \delta D\} + \{\delta Cr + \delta Sh + \delta PTloss\} \qquad (5.3\text{-}3)$$

The first grouping on the right hand side represents the constants over the time interval, and the second grouping lists the time-and/or-stress-dependent items.

Subsequent to the time-and-stress-dependent solution, for conformity with AASHTO requirements, at the end of each time-interval a second group of non-iterative solutions are obtained. These are explained next.

$$[A]\{ \delta u_{cr}\} = \{\delta Cr\} \qquad (5.3\text{-}4)$$

The solution to the Eqn. 5.3-4 yields the increment of displacement {δucr} due to increment of creep over the time interval. From the displacement increment {δucr} the associated stresses are computed. These represent the increment of stress in the structure due to creep. The total stress due to creep is obtained by summation of time-interval increments.

Likewise, for the contribution of shrinkage, the Eqn. 5.3-5 is used.

$$[A]\{ \delta u_{sh}\} = \{\delta Sh\} \qquad (5.3\text{-}5)$$

In the preceding procedure, the important point to note is that, the creep and shrinkage components are calculated by accounting for their full interaction with other components. In other words, the stresses reported due to creep recognize the shrinkage and prestressing losses that the structure undergoes. At a laboratory specimen level, it is customary to view the creep, shrinkage, and stress relaxation as independent phenomena. The same premise does not apply to the prototype. At the prototype level, creep induced stresses and the force in prestressing are significantly impacted by other time-dependent variables, such as shrinkage. The extraction procedure described herein accounts for the interaction of the different time elements.

An implicit requirement of AASHTO is the determination of actions due to prestressing alone. For Service Check load combinations, "Dead Load" includes prestressing and the associated prestress losses. In all the Strength Check load combinations, the hyperstatic (secondary) actions due to prestressing must be added with a load factor of 1. The hyperstatic actions are the actions induced in the structure due to constraint of the supports to free movement induced by prestressing and prestress losses. A full account of determination of hyperstatic actions is given by Aalami [Aalami, load balancing]. The actions due to prestressing are obtained from the following relationship.

$$[A]\{ \delta u_{pt}\} = \{\delta PT + \delta PTloss\} \qquad (5.3\text{-}6)$$

The incremental computation of actions due to prestressing ensures that secondary forces will appear only after the structure is made indeterminate. These will be due to additional and subsequent introduction of prestressing, or losses in prestressing forces of existing tendons.

In a similar manner to the preceding operations, the accumulative components of displacement and stress for dead loading (without prestressing) and temperature are computed from the following relationships:

For dead loading:

$$[A]\{ \delta u_F\} = \{\delta F\} \qquad (5.3\text{-}7)$$

For temperature:

$$[A]\{\delta u_T\} = \{\delta T\} \qquad (5.3\text{-}8)$$

6 - COMPOSITE CONSTRUCTION

A large percentage of segmentally-constructed bridges consist of prestressed precast girders with composite topping such as the example shown in Figs. 6.1-1 and 6.1-2. The application of high performance concrete, the combination of pre-. and post-tensioning in the girders, and the splicing of girders extend the application and analysis of these bridges beyond the traditional, simply-supported, single- span short bridge. In number, these bridges form the bulk of segmentally constructed structures.

The following reviews some of the important features in the structural modeling of these bridges as used in ADAPT [ADAPT, 1997].

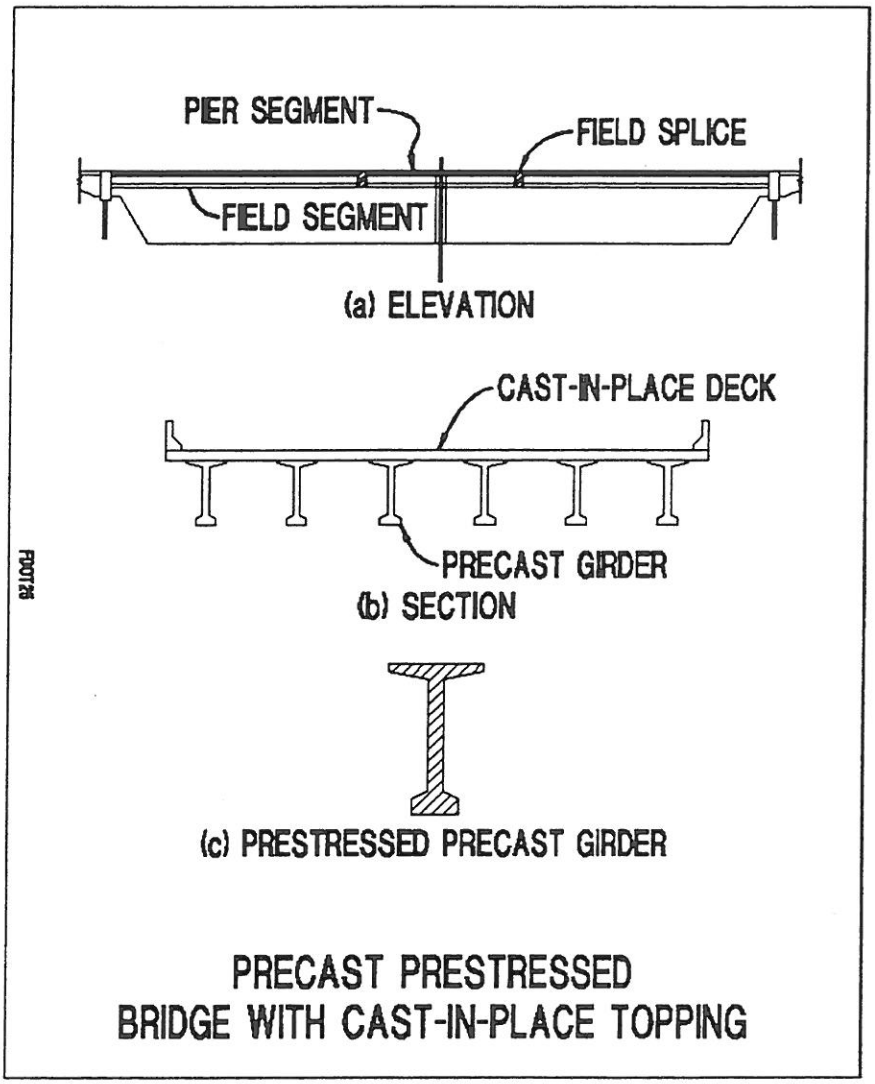

FIGURE 6.1-1

Refer to Fig. 6.1-3. The prestressed, precast girder shown is subdivided into elements, each with the concrete property of the precast girder. The topping slab is represented with elements matching in length to those of the girder. The elements of the topping are assigned with their respective age and concrete properties. The deformation at the ends of each element of topping slab are related to that of its associated precast girder element. The relationship of the two deformations imposes the assumption of plane sections remain plane over the entire cross-section of the bridge, thus forcing the girder and topping to deform in unison.

The modeling ensures the compatibility of displacement at the ends of each topping element. Sample examples run for spans divided into 20 elements have yielded accurate

solutions [adapt examples manual]. The accuracy of the solution can be controlled by the number of elements selected in each span for the topping.

Fig. 6.1-4 shows the actions on the topping and girder components of a section and their combination into the total sectional actions.

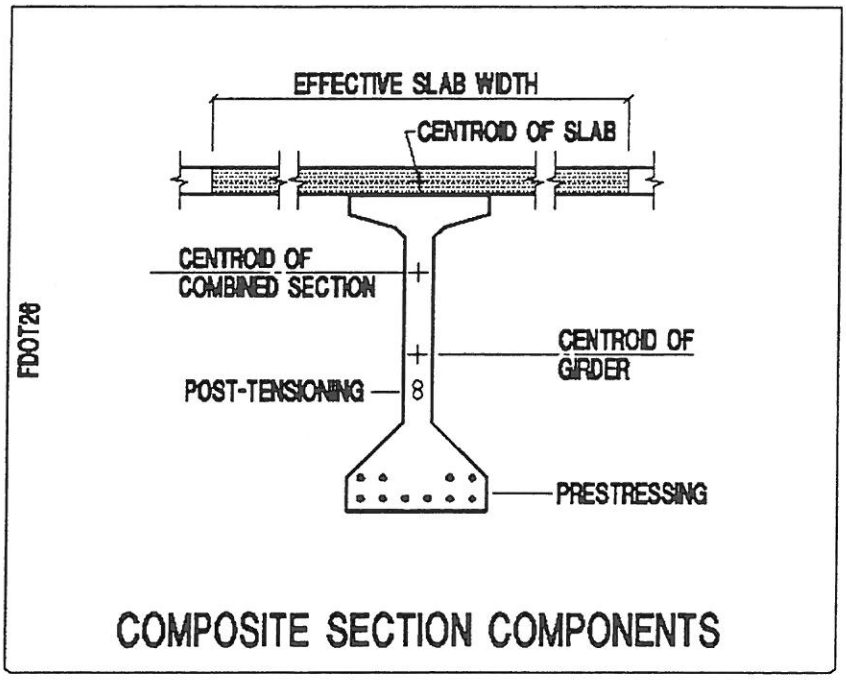

FIGURE 6.1-2

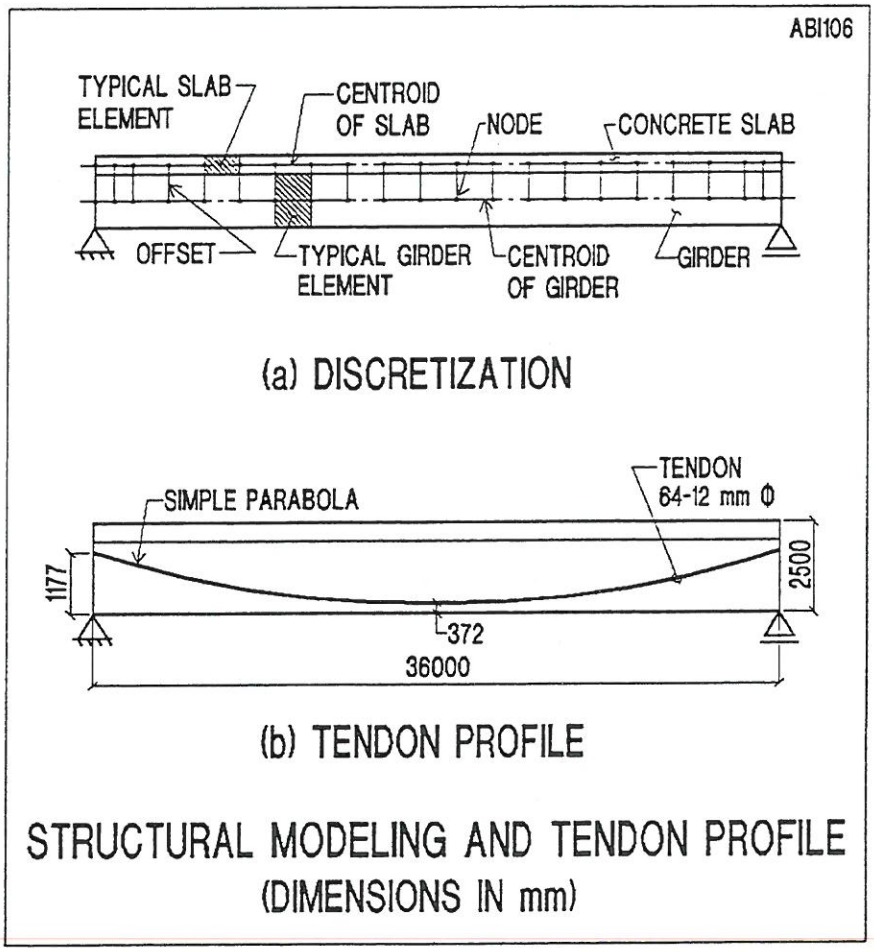
ABI106
TYPICAL SLAB ELEMENT
CENTROID OF SLAB
NODE
CONCRETE SLAB
OFFSET
TYPICAL GIRDER ELEMENT
CENTROID OF GIRDER
GIRDER
(a) DISCRETIZATION
SIMPLE PARABOLA
TENDON 64-12 mm Φ
1177
2500
372
36000
(b) TENDON PROFILE
STRUCTURAL MODELING AND TENDON PROFILE
(DIMENSIONS IN mm)

FIGURE 6.1-3

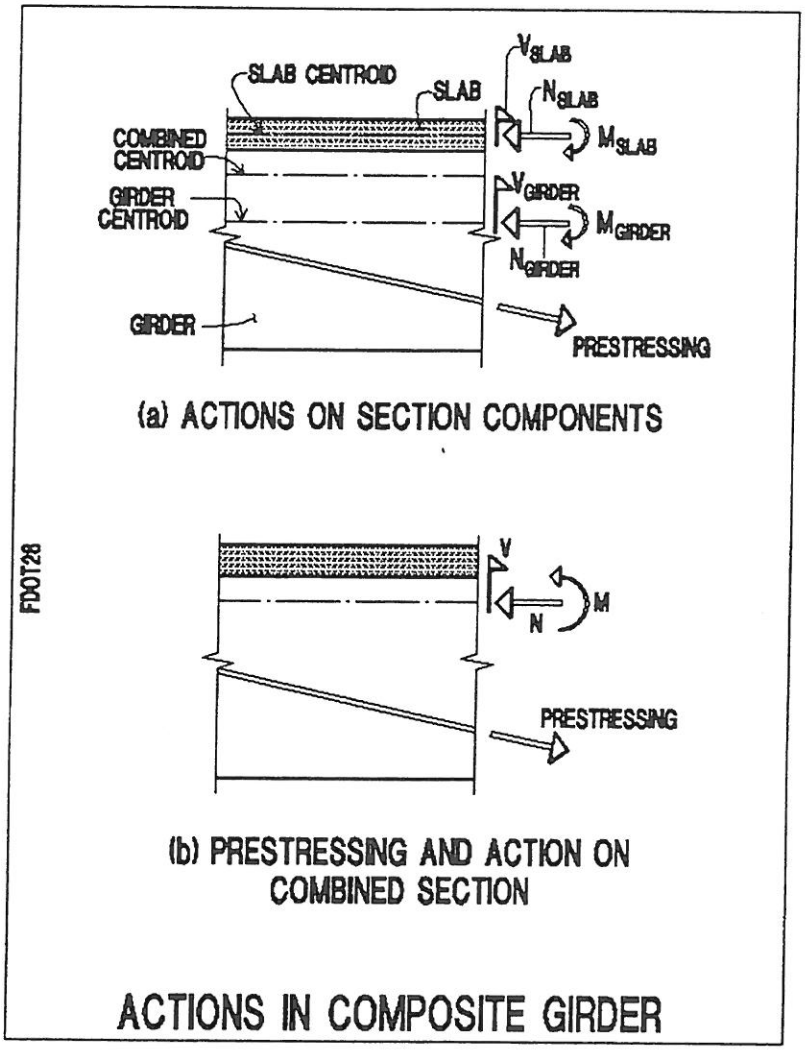

FIGURE 6.1-4

7 - EXAMPLE : TWO-SPAN SPLICED GIRDER

The following is an example of a two-span, spliced girder bridge made with precast, prestressed I-girders and cast-in-place topping. The example simulates one of the alternatives of the spliced girder bridge option under investigation at the California Department of Transportation.

7.1 Geometry and Construction Method

The layout and the overall dimensions of the bridge are illustrated in Fig. 7.1-1. The typical girder cross-section is shown in Fig. 7.1-2. The four precast girders are tied

together through a pier top girder (Fig. 7.1-3 (a) and (b)) and diaphragms over the end abutments. The bridge is constructed with span pier segments placed over the central pier (Fig. 7.1-4) and a precast segment for each span. The girders are spliced at 0.22 span from the central pier. There is no transverse diaphragm at the splices (Fig. 7.1-4) Tests conducted at University of California San Diego concluded that there is no significant advantage in forming a transverse diaphragm at the location of span splices for the geometry selected. [Holombo, 1995].

The position of the prestressing strands and the post-tensioning duct in the span-center segment and span-end segment are shown in Figs 7.1.5. Some of the prestressing strands are debonded over the pier in order to enable them to be cut and neutralized in the process of construction.

The sequence of construction envisaged for the bridge is illustrated in Fig. 7.1-6. The timetable and schedule is listed in Table 7.1-1

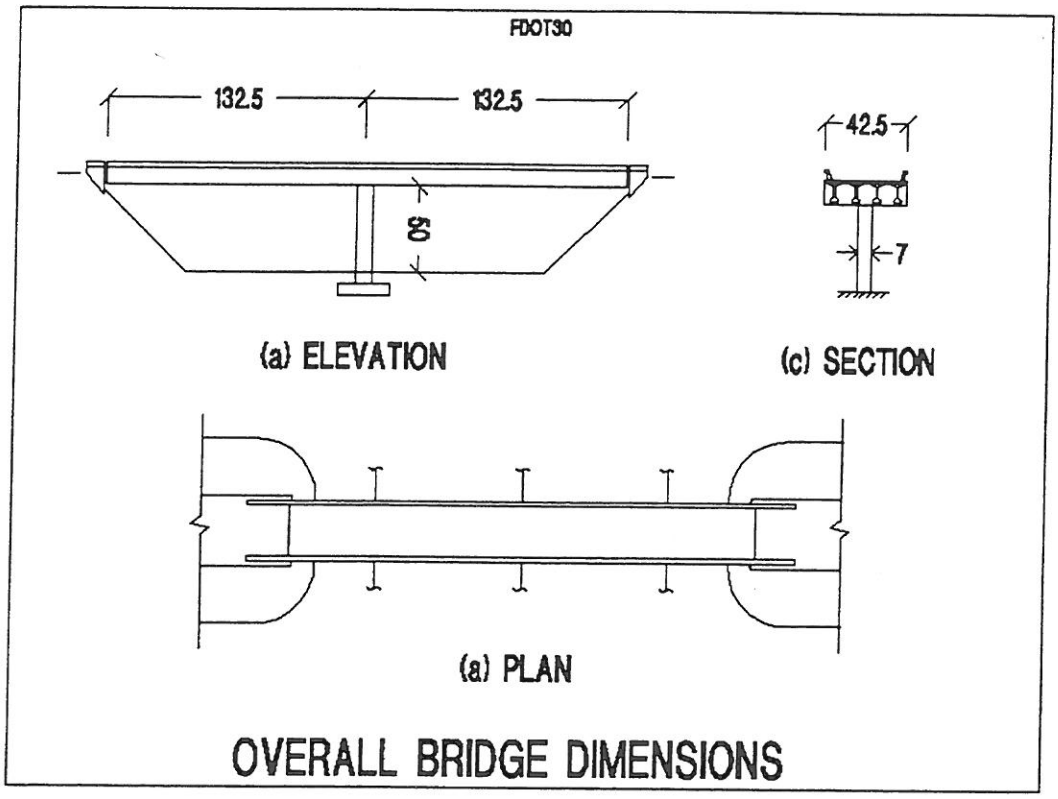

FIGURE 7.1-1

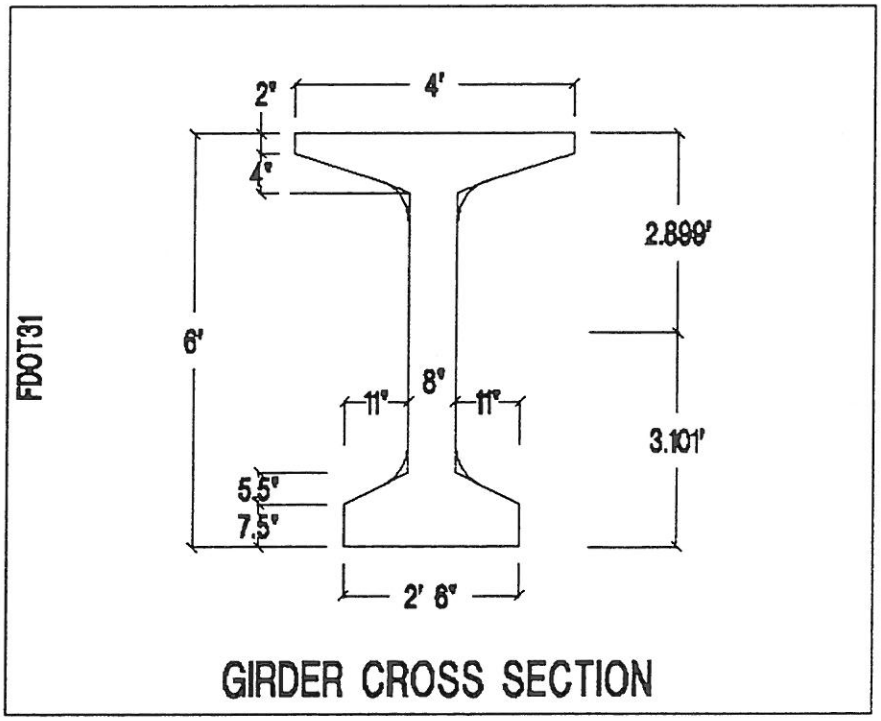

FIGURE 7.1-2

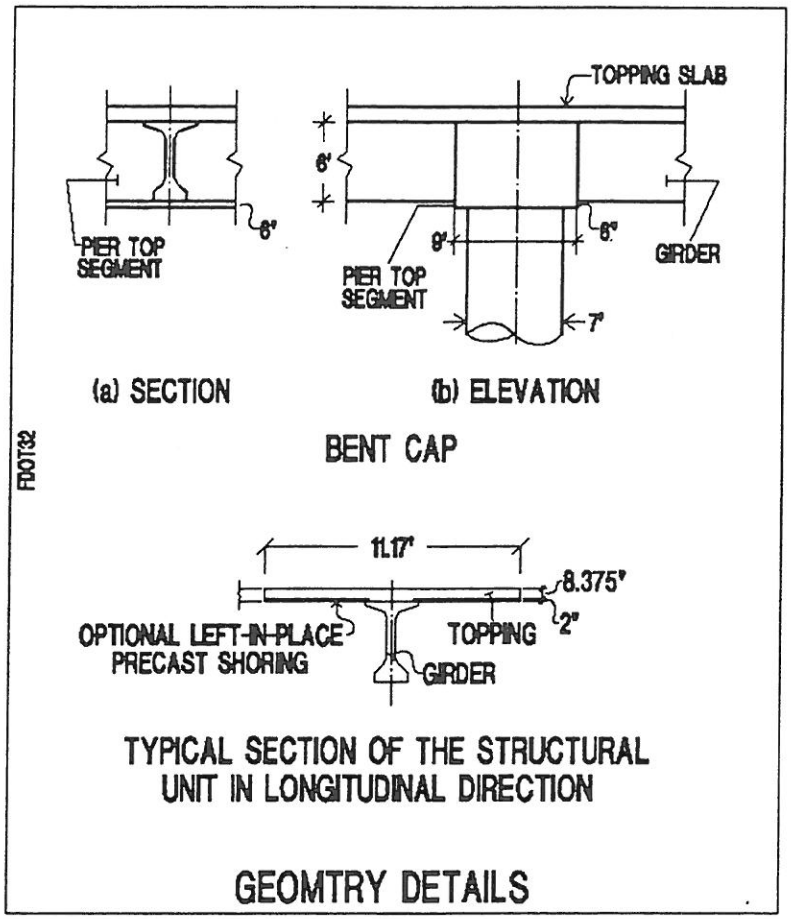

FIGURE 7.1-3

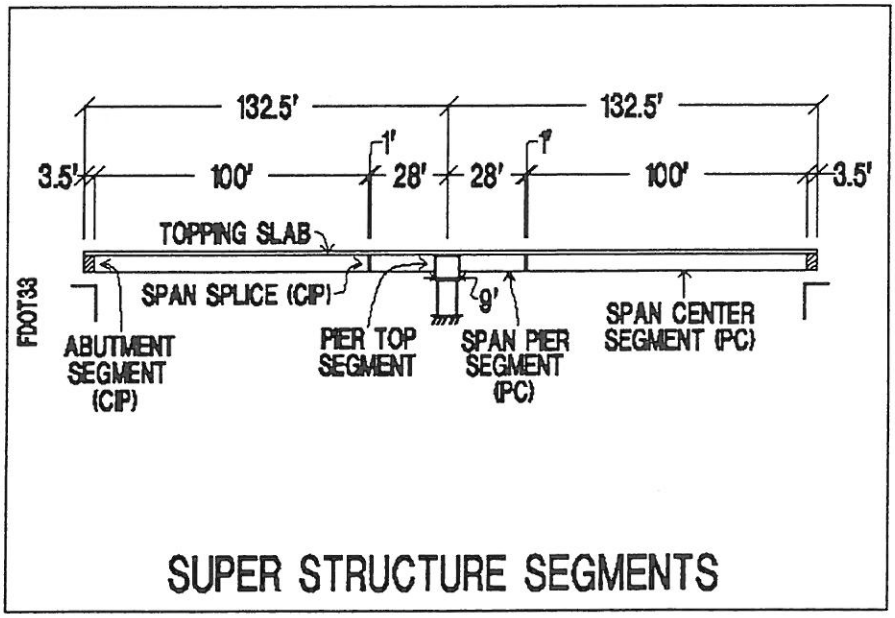

FIGURE 7.1-4

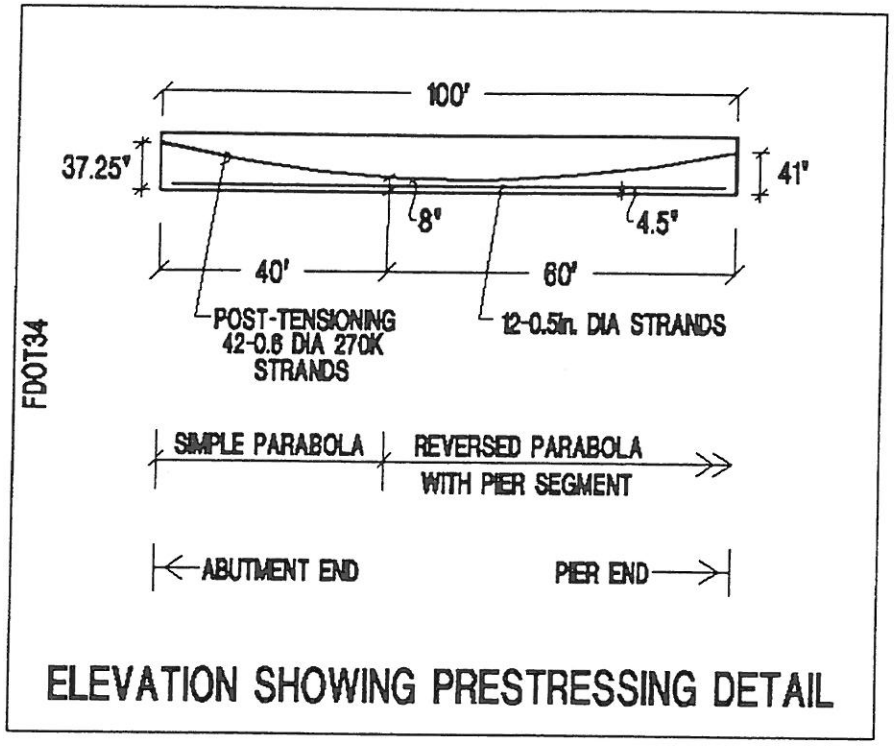

FIGURE 7.1-5-a

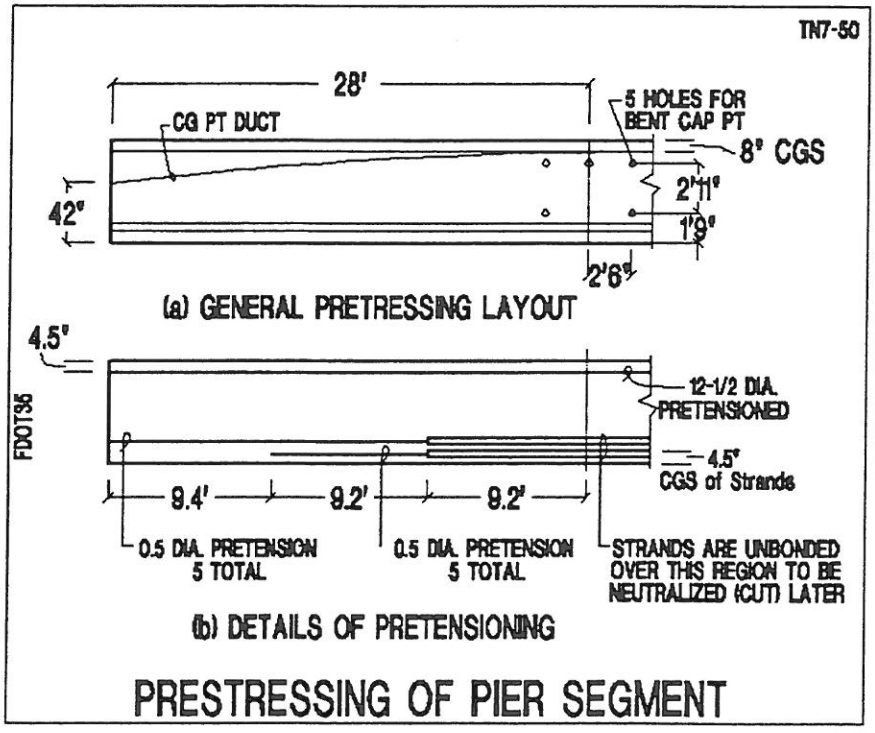

FIGURE 7.1-5-b

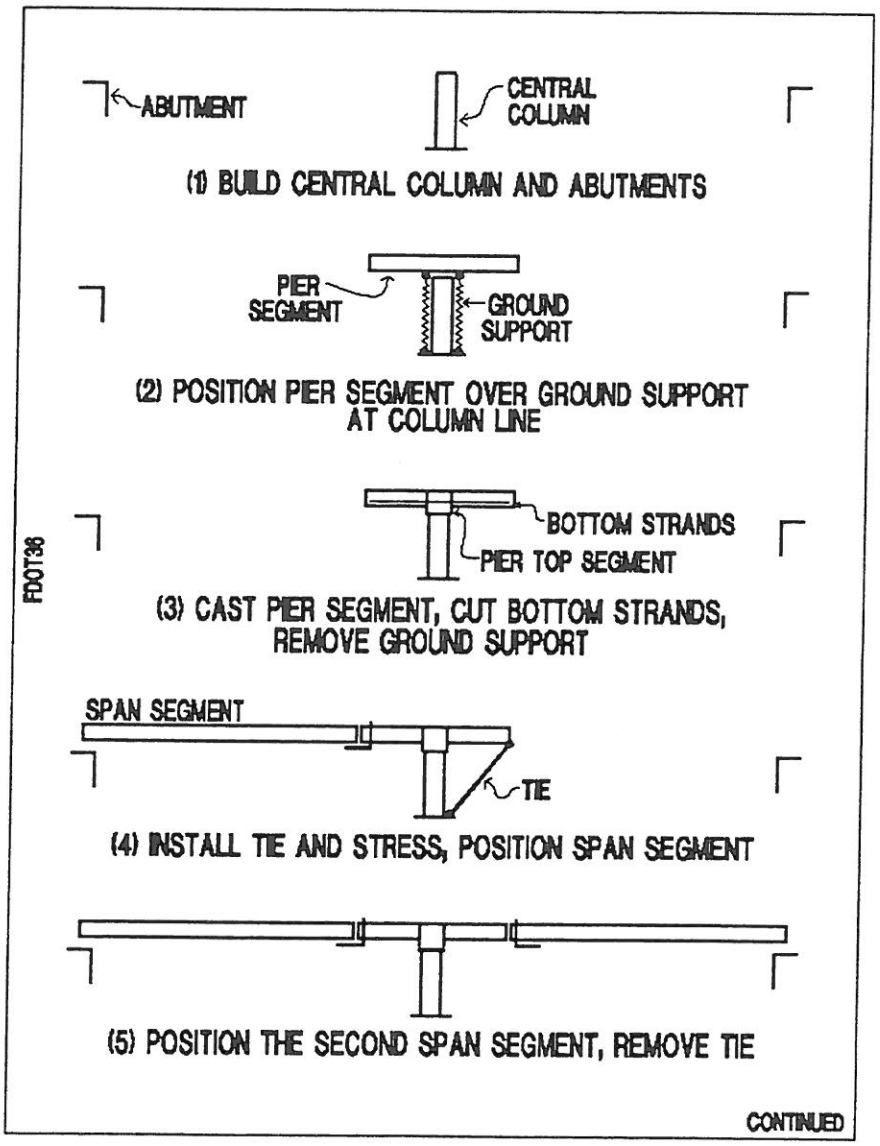

CONSTRUCTION SEQUENCE

FIGURE 7.1-6-a

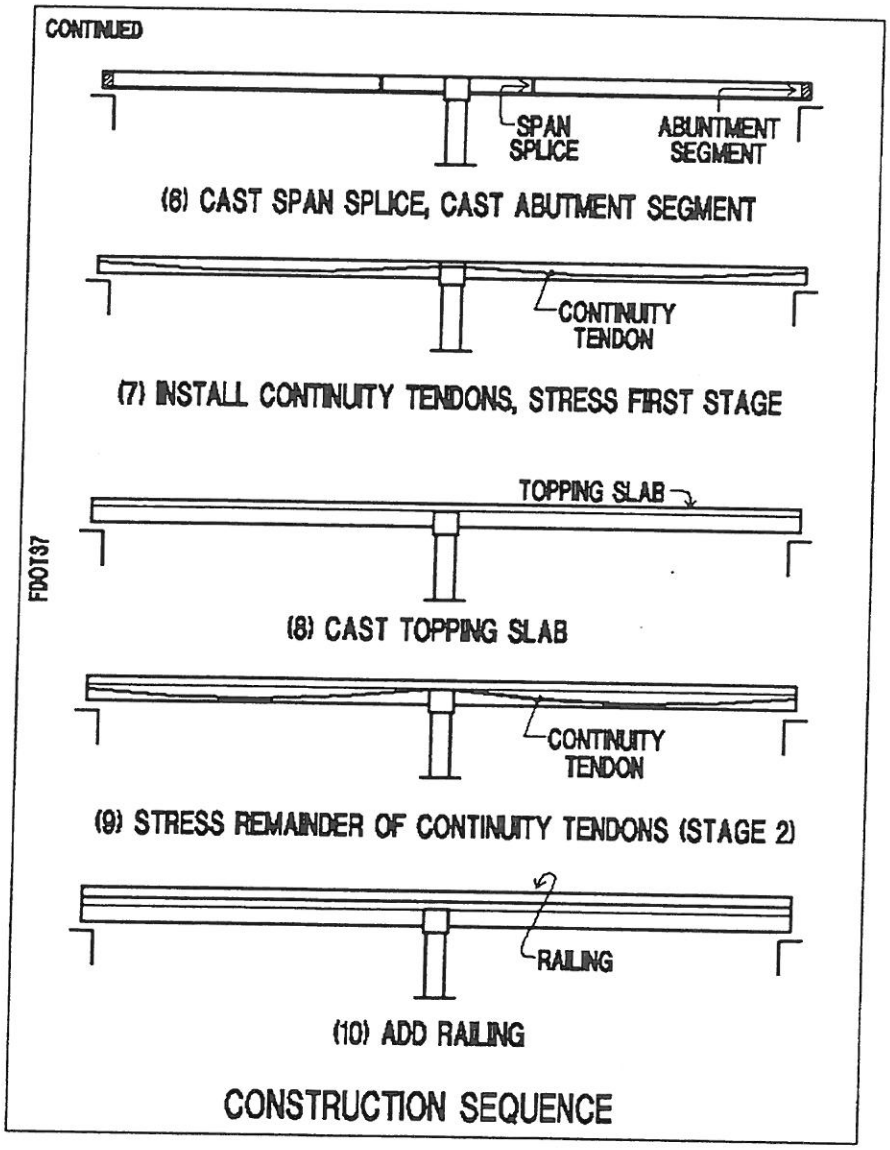
CONTINUED
SPAN SPLICE
ABUNTMENT SEGMENT
(6) CAST SPAN SPLICE, CAST ABUTMENT SEGMENT
CONTINUITY TENDON
(7) INSTALL CONTINUITY TENDONS, STRESS FIRST STAGE
TOPPING SLAB
FDOT137
(8) CAST TOPPING SLAB
CONTINUITY TENDON
(9) STRESS REMAINDER OF CONTINUITY TENDONS (STAGE 2)
RAILING
(10) ADD RAILING
CONSTRUCTION SEQUENCE

FIGURE 7.1-6-b

Table 7.1-1 lists the key events in the construction and the erection of the bridge. An erection scenario and schedule is assumed for the design of the bridge. Should the construction progress be different from that assumed in the analysis, the bridge would be analyzed while construction is in progress. If necessary, camber adjustments are made to those shown on the original drawings.

The number below the column "DAY" represents the lapse of days from time zero. The values in column "DURATION" are the estimated time between two successive events. This includes waiting time for curing, installation of form and reinforcement and other construction operations necessary before the next event can take place.

TABLE 7.1-1 TIMETABLE AND SCHEDULE OF CONSTRUCTION

EVENT	ACTION	COMMENT	DAY	DURATION (days)
1	Stress prestressing tendons		1	1
2	Cast concrete of span or pier segment	(1)	1	0
3	Release prestressing strands		3	2
4	Remove girders from bed		4	1
5	Store girders in yard	(2)	18	14
6	Cast footing, column and abutments	(3)		
7	Transport and position pier segment over ground support adjacent to central column			3
8	Cut bottom strands of pier segment			1
9	Cast pier top segment (bent cap)			1
10	Stress transverse tendons in bent cap; remove shoring	(4)		1
11	Install tie on one side and stress taut			
12	Secure span segment in position on span with no tie	(5)		1
13	Position the second side's span segment			1
14	Place tendon duct splices through the span splice and abutment segment	(6)		
15	Cast span splice and abutment segment			4
16	Place the continuity post-tensioned tendons; stress stage 1			2
17	Place topping slab			2
18	Stress the remainder of continuity tendons			1
19	Add railing and other superimposed dead weight			1

Comments:

(1) Due to different pretensioning reinforcement, span and pier segments will be cast separately
(2) Girders will be supported on two points each, at a support position to be determined.
(3) In the design example, the lower end of the column is assumed as fixed to the foundation. The footing or pile cap are not modeled.
(4) The prestressing in the transverse direction to the girder (along the bent cap) is not modeled for the longitudinal analysis. Its stressing event is used to determine the time the support below the bent cap is neutralized.
(5) Span segment's weight supported on the abutment and bracket at end of pier segment.
(6) The operation does not impact the modeling for the bridge analysis and design

7.2 Material Properties

The material properties of the bridge are as follows:

7.2.1 Concrete

- f'c beam = 6000 psi (41 MPa)
- f'c topping = 4000 psi (26 MPa)
- Unit weight = 150 pcf (2400 kg/m^3)
- Alpha = 0.000006 /degree Fahrenheit (Coefficient of thermal expansion)
- Creep Characteristics = based on ACI -206 (AASHTO)
- Creep Coefficient = 1.8
- Shrinkage Characteristics = based on ACI -206 (AASHTO)
- Shrinkage Coefficient = 0.00048

7.2.2 Nonprestressed Steel

- Es = 29000 ksi (2.0E5 MPa)
- Percentage of reinforcement in concrete = 1% in girder and topping
  = 3% in splices

7.2.3 Prestressing Steel

A - Strand Properties

- As = 0.217 in^2 (140.0 mm^2), 0.60" nominal diameter for pretensioning; 0.153 in^2 (98.8 mm^2) for post-tensioning; both 7-wire strands
- Strand type = low relaxation (R=45)
- Fpu = 270 ksi (1860 MPa)
- Esp = 28000 ksi (1.93E5 MPa)
- Alpha = 0.000006 /degrees Fahrenheit (Coefficient of thermal expansion)

B - System Parameters

- Coefficient of angular friction for prestress = 0.0 /radian
- Coefficient of wobble friction for prestress = 0 / in
- Coefficient of angular friction for post-tensioning = 0.25/radian

- Coefficient of wobble friction for post-tensioning = 0.0003 / in (1.18E-5/mm)

C - Stressing

- fpi for prestress = 0.75 Fpu
  = 202.5 ksi (1400 MPa)
- Anchor set for prestress = 0 in
- fpi for post-tensioning = 0.80 Fpu
  = 202.5 ksi (1400 MPa)
- Anchor set for post-tensioning = 3/8 in (9.5 mm)

7.3 Structural Modeling

The precast girder, the short splice, the slab topping, the abutment and pier head girders were all modeled separately. Details of their geometry are illustrated in Fig. 7.3-1.

The debonded (wrapped) portions of the prestressing strands were modeled as unbonded tendons. The transfer of force between prestressing strands and the girder is effected over the bonded length of prestressing strands.

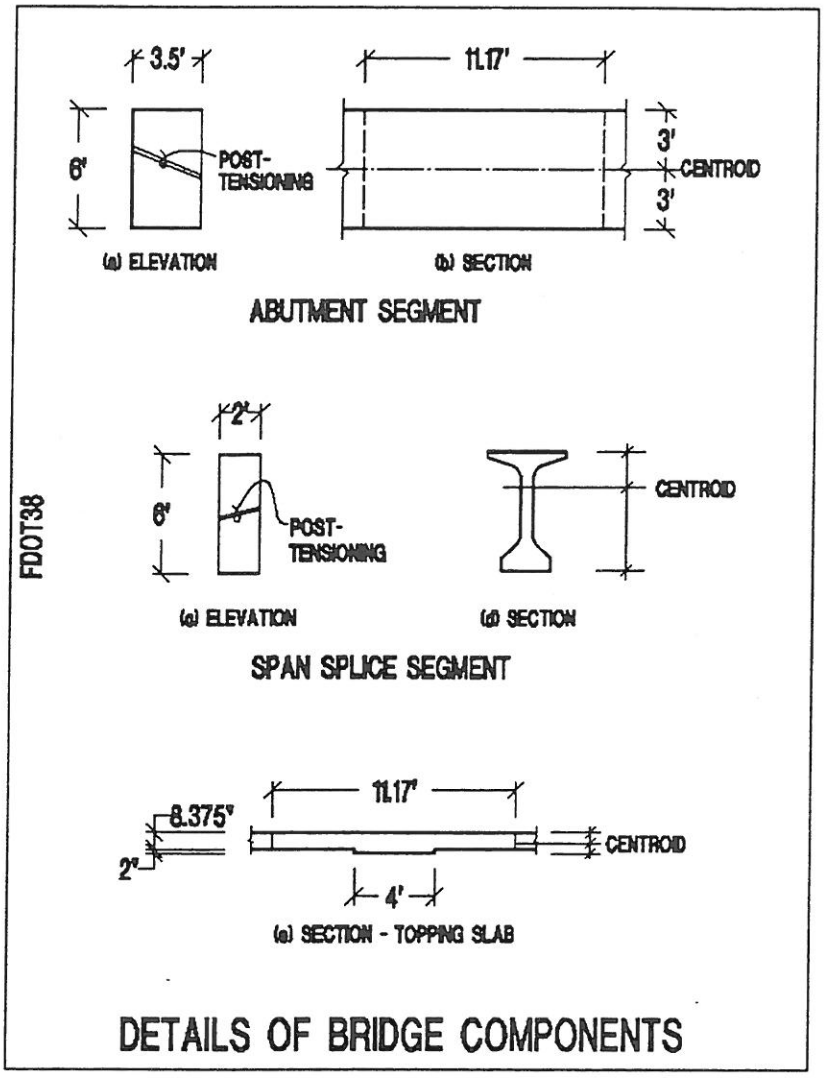

FIGURE 7.3-1

At the interface between the girders and diaphragms (at the central pier and at the abutments), the shift in position of the centroid of the diaphragms with respect to that of the girder results in the introduction of concentrated moments from the prestressing in the girders. To capture the impact of this moment in the response of the structure, the elements of the girder and diaphragm were modeled with an offset as illustrated in Fig. 7.3-2.

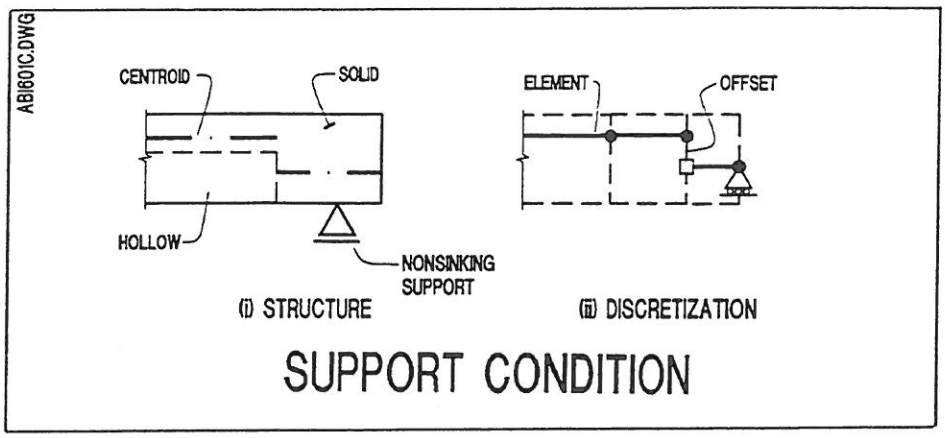

FIGURE 7.3-2

7.4 Analysis

The analysis was performed for the construction of the bridge starting from the stage when the girders were cast in the precasting yard, through twenty years after the completion of the construction. Some of the typical results obtained are illustrated in the following graphics.

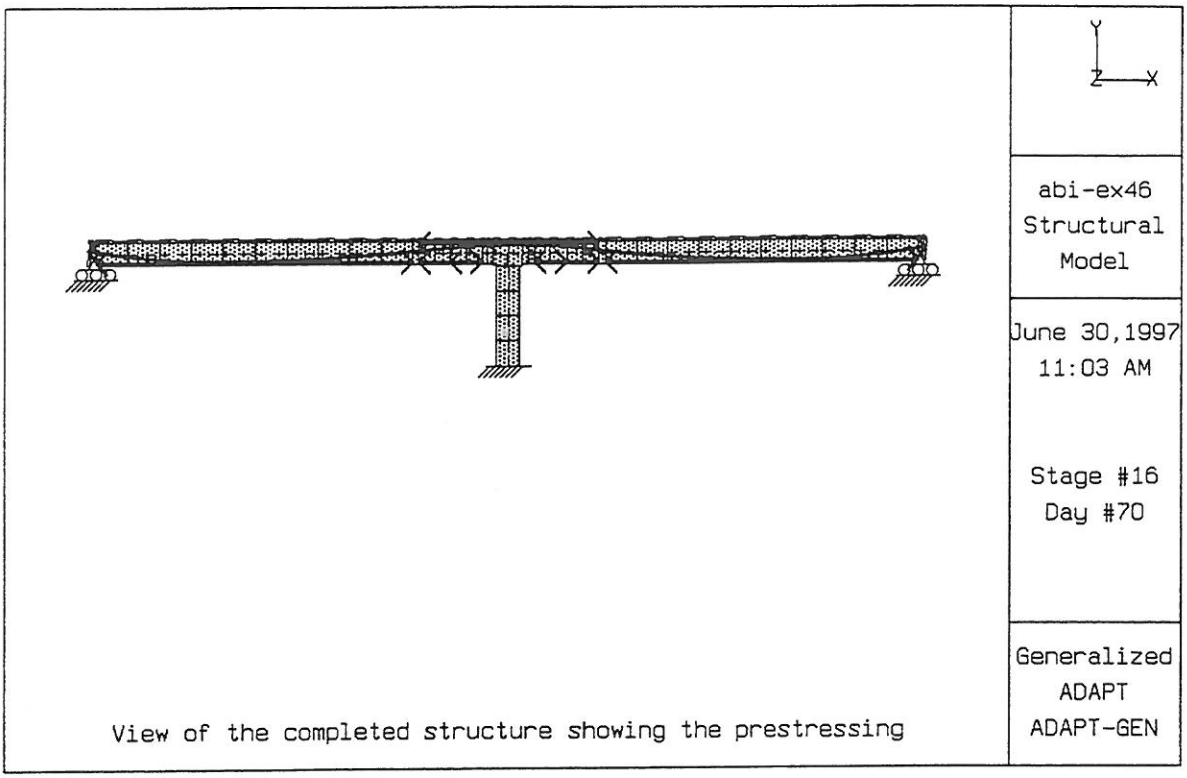

View of the completed structure showing the prestressing

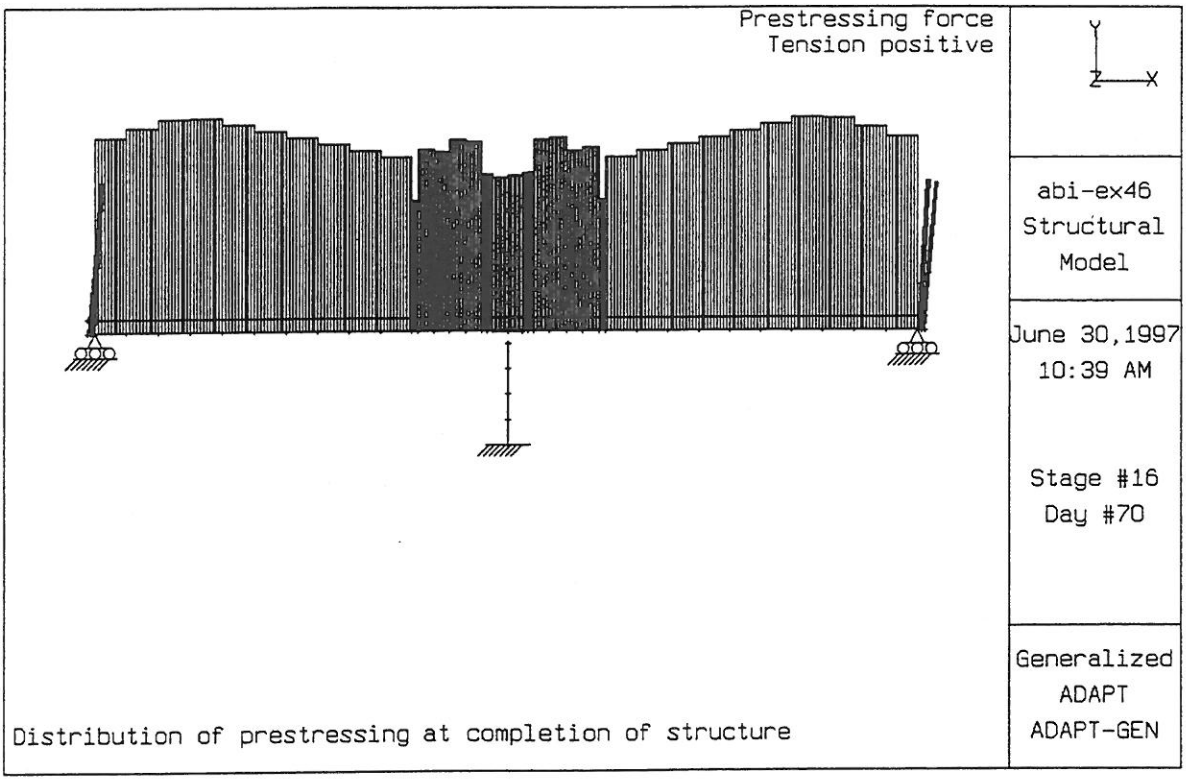

Distribution of prestressing at completion of structure

DISPLAY OF TYPICAL ANALYSIS RESULTS

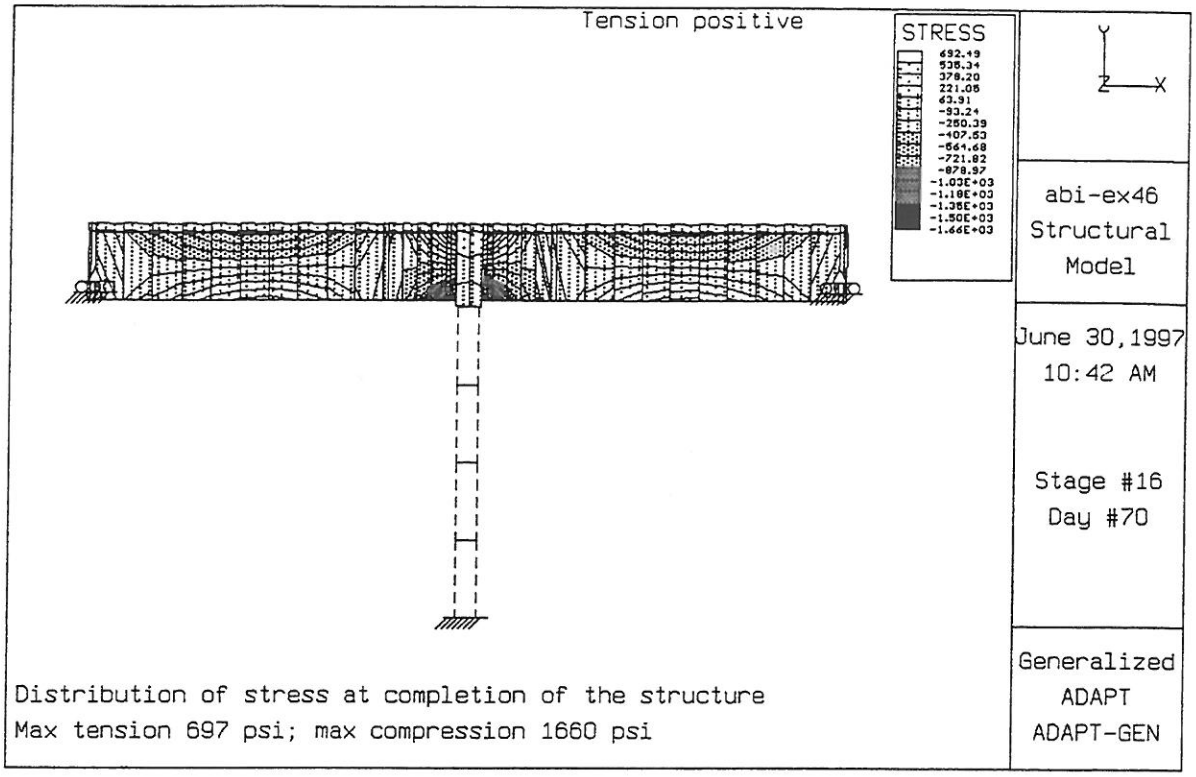

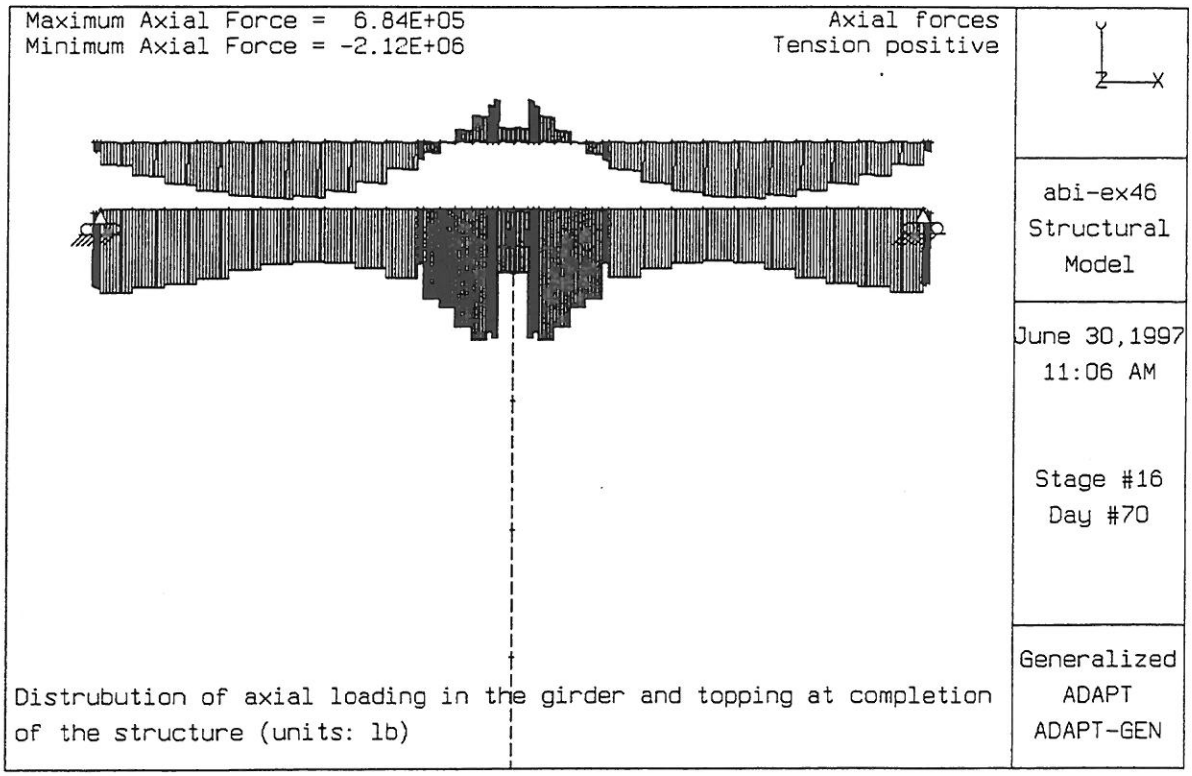

DISPLAY OF TYPICAL ANALYSIS RESULTS

8 - CONCLUDING REMARKS

Accurate prediction of material and construction, time-dependent parameters are critical for a successful completion of segmentally erected prestressed concrete bridges. Current technological advances allow full recognition and implementation of time dependent parameters for construction of special types of structures in which camber, alignment and stress control are required. In this context, AASHTO recognizes the need for special treatment of segmentally designed bridge structures. An explicit methodological approach and recommendations are still lacking. Covering the topics listed below, this work attempts to answer several critical questions in the analysis and design of segmentally constructed bridges.

The work describes the features of segmentally constructed bridges and the principal considerations for their design. The impact of time-dependent parameters creep, shrinkage, aging of concrete, relaxation in prestressing and the interaction among them are detailed. Procedures for the inclusion of the time-dependent parameters in the design are presented and discussed.

Application of laboratory tests for analysis and design of bridges constructed with high performance concrete and early-age loading is outlined.

In conformance with AASHTO requirements, a method is offered to account for the extraction of stresses and deformations in segmental bridge construction due to each of the time-dependent parameters.

An example of a precast, prestressed girder bridge with topping is used to illustrate the items discussed.

9 - REFERENCES

Aalami, Bijan, O. (1993),"*Design and Analysis of Segmentally Constructed Brides*," Proceedings, CONCET'93, International Conference on Engineering and Technology, Kuala Lumpur, Malaysia, May 25-27, 1993, pp. TS2-1,16, 1993.

Aalami, Bijan, O. (1990)," Load Balancing - A comprehensive Solution to Post-Tensioning," Structural Journal, ACI, November-December 1990, pp. 662-670, 1990.

AASHTO (1996), "*AASHTO Standard Specifications for Highway Bridges*," 16th edition, Washington, DC, pp.760, 1996.

AASHTO (1994), "*AASHTO LRFD Bridge Design Specifications*," Washington, DC, pp.1116, 1994.

AASHTO, (1989) "*Guide specifications for design and construction of segmental concrete bridges*," American Association of State Highway and Transportation Officials, Washington, D.C., pp. 118.

ACI Committee 209, (1982), "*Prediction or creep, shrinkage and temperature effects in concrete structures*," ACI-209R-82, American Concrete Institute.

ADAPT-ABI , (1997) " *ADAPT software Manuals for analysis and design of incrementally constructed bridges*", ADAPT, 1733 Woodside Road, No 220, Redwood City, Ca 94061, 1997.

CEB-FIP, (1990)"*CEB-FIP model code for concrete structures,*" Comite Euro-International de Beton, Thomas Telford, England, 1990.

CEB-FIP, (1978) "*CEB-FIP model code for concrete structures,*" Comite Euro-International de Beton, Lewis Brooks, 2 Blagdon Rd, New Malden, Surrey, KT3 4AD, England.

Hernandez, H. D. and Gamble, E. L., (1975) "Time dependent prestress losses in prestressing concrete construction," Structural Research Series N0 417, Civil Engineering Studies, University of Illinois, Urbana, May 1975.

Holombo, J. (1995), "Large Scale Testing of Precast-Spliced Girder Bridges," PCMAC Publication, Glendale, Ca., also, University of California, San Diego, October 1995.

Kabir, A. F., (1976),"*Nonlinear analysis of reinforced concrete panels, slabs and loading*," University of California at Berkeley, SESM Report No 76-6, 1976.

Khan, A. A., Cook, W. D., and Mitchell, D., (1977), "*Creep, Shrinkage, and Thermal Strains in Normal, Medium and High-Strength Concrete during Hydration*," American Concrete Institute Material Journal, March-April 1997, pp. 156-163.

Magura, D. D., Sozen, M. A. and Seisss, C. P. (1964), "*A Study of Stress Relaxation in Prestressing Reinforcement*," PCI Journal, Vol. 9, No.2, April 1964.

Mokaddam, M. A., (1969), " *Behavior of concrete under variable temperature and loading*", Interim Report to Oakridge National Laboratory, Reactor Division, Oakridge, Tennessee.

PCI Committee on Segmental Construction, (1975) "*Recommended practice for segmental construction in prestressed concrete*," PCI, pp.22 - 41, 1975.

PCI Bridge Committee , (1975) "*Tentative design and recommendation specifications for precast segmental box girder bridges*," PCI Journal, pp. 34-42, Jul-Aug.

PCI, (1985), "PCI Design Handbook," Prestressed Concrete Institute, Chicago, Il, pp. approx. 600.

Tadors, M.K., Ghali, A. and Dilger, W., (1975) "*Time-dependent prestress loss and deflection in prestressed concrete members*," PCI Journal, Vol. 20, No. 3, May-June, 1975.

ACKNOWLEDGMENT

The author wishes to record his appreciation to Mr Jess Avila of California Department of Transportation for his contribution in the development of the spliced girder bridge example, and Dr Jian Tao for his contribution in the analytical of the AASHTO required time-dependent stresses.